

## Research Article

# Symbiosis with Dinoflagellates Alters Cnidarian Cell-Cycle Gene Expression

Lucy M. Gorman <sup>1</sup>, Migle K. Konciute <sup>2</sup>, Guoxin Cui <sup>2</sup>, Clinton A. Oakley <sup>1</sup>,  
Arthur R. Grossman <sup>3</sup>, Virginia M. Weis <sup>4</sup>, Manuel Aranda <sup>2</sup> and Simon K. Davy <sup>1</sup>

<sup>1</sup>School of Biological Sciences, Victoria University of Wellington, Wellington 6140, New Zealand

<sup>2</sup>Red Sea Research Center, Division of Biological and Environmental Science and Engineering (BESE), King Abdullah University of Science and Technology (KAUST), Thuwal 23955-6900, Saudi Arabia

<sup>3</sup>Department of Plant Biology, The Carnegie Institution for Science, Stanford, California 94305, USA

<sup>4</sup>Department of Integrative Biology, Oregon State University, Corvallis, Oregon 97331, USA

Correspondence should be addressed to Manuel Aranda; [manuel.aranda@kaust.edu.sa](mailto:manuel.aranda@kaust.edu.sa) and Simon K. Davy; [simon.davy@vuw.ac.nz](mailto:simon.davy@vuw.ac.nz)

Received 21 February 2022; Accepted 16 April 2022; Published 23 May 2022

Academic Editor: Jayaprakash Kolla

Copyright © 2022 Lucy M. Gorman et al. This is an open access article distributed under the Creative Commons Attribution License, which permits unrestricted use, distribution, and reproduction in any medium, provided the original work is properly cited.

In the cnidarian-dinoflagellate symbiosis, hosts show altered expression of genes involved in growth and proliferation when in the symbiotic state, but little is known about the molecular mechanisms that underlie the host's altered growth rate. Using tissue-specific transcriptomics, we determined how symbiosis affects expression of cell cycle-associated genes, in the model symbiotic cnidarian *Exaiptasia diaphana* (Aiptasia). The presence of symbionts within the gastrodermis elicited cell-cycle arrest in the G<sub>1</sub> phase in a larger proportion of host cells compared with the aposymbiotic gastrodermis. The symbiotic gastrodermis also showed a reduction in the amount of cells synthesizing their DNA and progressing through mitosis when compared with the aposymbiotic gastrodermis. Host apoptotic inhibitors (Mdm2) were elevated, while host apoptotic sensitizers (c-Myc) were depressed, in the symbiotic gastrodermis when compared with the aposymbiotic gastrodermis and epidermis of symbiotic anemones, respectively. This indicates that the presence of symbionts negatively regulates host apoptosis, possibly contributing to their persistence within the host. Transcripts (ATM/ATR) associated with DNA damage were also downregulated in symbiotic gastrodermal tissues. In epidermal cells, a single gene (Mob1) required for mitotic completion was upregulated in symbiotic compared with aposymbiotic anemones, suggesting that the presence of symbionts in the gastrodermis stimulates host cell division in the epidermis. To further corroborate this hypothesis, we performed microscopic analysis using an S-phase indicator (EdU), allowing us to evaluate cell cycling in host cells. Our results confirmed that there were significantly more proliferating host cells in both the gastrodermis and epidermis in the symbiotic state compared with the aposymbiotic state. Furthermore, when comparing between tissue layers in the presence of symbionts, the epidermis had significantly more proliferating host cells than the symbiont-containing gastrodermis. These results contribute to our understanding of the influence of symbionts on the mechanisms of cnidarian cell proliferation and mechanisms associated with symbiont maintenance.

## 1. Introduction

Coral reefs are one of the most negatively impacted ecosystems on our planet [1], a consequence of anthropogenic climate change that has led to ocean warming and acidification [2, 3]. Reef-building scleractinian corals and other

cnidarians (soft corals, sea anemones, jellyfish, and hydrocorals) form symbioses with dinoflagellates of the family Symbiodiniaceae [4], which are located in the host's gastrodermal cells within host-derived vacuolar compartments known as "symbiosomes" [5, 6]. During stable environmental conditions, this symbiosis is mutualistic, with the

major benefit being the exchange of nutrients [7]. In particular, fixed carbon is translocated from the algae to the host, predominantly in the form of glucose [8, 9], while inorganic nitrogen is released to the algae by the host [10, 11]. This nutritional interplay underlies the success of coral reefs in nutrient-poor tropical waters [12].

Evolved interactions between the resident symbiont and the host are integral for controlling the metabolic integration, nutritional state, and coordinated growth of the symbiont and host [13]. The host has evolved several homeostatic mechanisms to regulate the steady-state symbiont density, including premitotic mechanisms such as cell-cycle arrest [14, 15] and postmitotic mechanisms such as autophagy [16, 17], apoptosis [17–19] and expulsion [20–23]. These host regulatory processes have been shown to be upregulated when conditions favour symbiont growth and/or are suboptimal for the host, e.g., increased temperatures [17, 20, 24–26], or the host associates with heterologous (i.e., nonnative) symbiont types [18].

Cell-cycle control has been proposed as one of the dominant mechanisms for regulating symbiont biomass in the cnidarian-dinoflagellate symbiosis, with the arrest of the cell cycle of the majority of symbionts in the  $G_1/S$  phase, compared with symbionts in culture [14, 27]. The mitotic cell cycle is a biological process that allows eukaryotic organisms to renew, repair and grow their tissues [28–30]. It involves a first gap phase ( $G_1$ ) where cells grow [31], a DNA synthesis phase (S) where DNA is replicated [32], a second gap phase ( $G_2$ ) where DNA damage is repaired before mitosis [33], and finally a mitotic phase (M) where cells divide [34]. Checkpoints within the specific cell-cycle phases control cell proliferation under unfavourable environmental conditions and prevent damaged cells from propagating [15].

Coordination of host and symbiont growth is vital for maintaining optimal functioning between the biological partners in a dynamic environment (both biotic and abiotic), which can shift the metabolic equilibrium and help sustain the association. The symbiotic state elicits proliferation of host cells in both the epidermis and gastrodermis, with proliferation most pronounced in host cells closest to the symbionts ( $<13\ \mu\text{m}$ ) [27]. In contrast, reduced proliferation of symbiont cells *in hospite* during colonization (compared with log phase growth in culture) appears to be the result of altered progression of the symbiont cell cycle through arrest of the symbionts in the S phase, which causes fewer cells to enter the  $G_2/M$  phase and thus divide [27]. It is unclear whether the proportion of the symbiont population within the different phases of the cell cycle changes after the symbionts reach a steady-state population in the host. In the hydroid *Myrionema ambionense*, measurement of the mitotic index *via* light microscopy indicated that symbiont biomass becomes synchronized with the biomass of the host once the symbiont population reaches a steady state [35]. For instance, *M. ambionense* host cells were observed dividing after host feeding and the symbiont cells divided 10–12 hours following host cell division, but only if given access to ample light [35].

The molecular mechanisms that underlie host-symbiont coordination and synchrony are only now being described. Previous transcriptomic studies have shown that the symbiotic state changes the expression of 920 and 91 host genes in the sea anemones *Exaiptasia diaphana* (= *E. pallida*; commonly referred to as “Aiptasia”) [36] and *Anthopleura elegantissima* [37], respectively. Furthermore, the symbiotic state also caused a shift in the rhythms of host gene expression in Aiptasia, with 10% of genes changing their periodicity from 12- to 24-hour rhythms [38]. In this latter study, one of the top five canonical pathways that changed its periodicity was the mammalian target of rapamycin (mTOR) pathway. This pathway combines nutrient and mitogenic signals to integrate cell growth/size [39, 40], an important factor when determining progression through cell-cycle checkpoints [41]. In *A. elegantissima*, the presence of symbionts resulted in a decrease in the expression of four host genes involved in host cell apoptosis and an increase in the expression of one host gene involved in host cell proliferation through an impact on the sphingosine-1-phosphate (S1P) and prohibitin pathways [37]. In Aiptasia, S1P has been shown to promote host cell survival both during association with symbionts [42] and periods of host stress [43]. However, we still have a long way to go to understand which host genes are altered in their expression in the presence of symbionts and how this induces downstream effects on host growth.

The development of the Aiptasia model system and the advancement in “omic” technologies has played a significant role in describing the molecular differences in the cnidarian host induced by the establishment of the symbiotic state [36, 38, 44–47]. We expanded on these pioneering studies to further our understanding of cell-cycle regulation in the cnidarian-dinoflagellate symbiosis, by analyzing a cnidarian tissue-specific transcriptomic dataset that compares differences in expression of host cell-cycle genes between symbiotic states (aposymbiotic *versus* symbiotic) and host tissue types (epidermis *versus* gastrodermis). We confirmed the identity of Aiptasia genes by bioinformatics using phylogenetic analysis. Following the findings of the gene expression changes, a microscopy method was developed to quantify the number of proliferating host cells in the gastrodermis and epidermis of Aiptasia when in the aposymbiotic state (i.e., symbiont free) and when recently inoculated with symbiotic dinoflagellates (two days postinoculation) and in the fully established symbiotic state.

## 2. Methods

### 2.1. Tissue-Specific Transcriptomics

**2.1.1. Animal Maintenance and Laser Microdissection.** Aposymbiotic anemones for this experiment were obtained by bleaching symbiotic anemones *via* cold-shock treatment in combination with the photosynthetic inhibitor diuron (Sigma-Aldrich) [48, 49]. After removal of symbionts, aposymbiotic animals were kept under the same conditions as the symbiotic anemones for at least three months. To ensure the absence of symbionts, anemones were examined for the

presence of chlorophyll *a* autofluorescence once a week and on the day of the experimental setup using a fluorescence microscope (Leica DMI3000 B) at  $\times 10$  magnification. Afterwards, symbiotic and aposymbiotic *Aiptasia* (strain CC7) were kept in replicate-specific tanks containing autoclaved seawater from the Red Sea with salinity adjusted to  $\sim 37$  ppt. Tanks were kept on a 12 h:12 h light:dark cycle with  $\sim 40 \mu\text{mol photons m}^{-2}\cdot\text{s}^{-1}$  of photosynthetically active radiation and fed with freshly hatched *Artemia* sp. brine shrimp nauplii approximately three times *per week*. One anemone from each tank was collected after six hours in the light, snap frozen in liquid nitrogen immediately, and embedded with tissue freezing medium (Electron Microscopy Sciences, USA). The embedded samples were stored at  $-80^\circ\text{C}$  before cryosectioning.

The cryostat (Leica Biosystems, Germany) was pre-chilled to a chamber temperature of  $-23^\circ\text{C}$ . Samples were equilibrated to the chamber temperature for 20 min, and then, for each replicate, a layer of tissue was cut from the top to the bottom of the animal and dissected at a thickness of  $8 \mu\text{m}$ . Tissue sections were placed on microscope slides (1–3 *per slide*), and the gastrodermis and epidermis were identified using a Leica LMD 6000 microscope (Leica Microsystems, Germany) and a Leica filter cube B/G/R and A (Leica Microsystems, Germany). Regions of interest were traced by LMD software and dissected using the ultraviolet laser beam. The dissected tissues were collected in caps containing  $40 \mu\text{L}$  RNA extraction buffer from an Arcturus PicoPure RNA Isolation Kit (Thermo Fisher Scientific, USA). The harvested cells were lysed at  $42^\circ\text{C}$  for 30 min, vortexed briefly, and then kept at  $-80^\circ\text{C}$  until further processing.

**2.1.2. Tissue-Specific RNA-Seq.** Total RNA from the cell lysates was extracted using an Arcturus PicoPure RNA Isolation Kit following the protocol for use with CapSure Macro LCM Caps. The quality of RNA samples was assessed using an Agilent RNA 6000 Pico Kit with an Agilent 2100 Bioanalyzer (Agilent Technologies, USA). cDNA was synthesized using an Ovation RNA-seq System V2 Kit (NuGen, USA) following the manufacturer's instructions. The amplified cDNA was processed for library preparation using a NEBNext Ultra II DNA Library Prep Kit (NEB, USA) for Illumina sequencing. The samples were pooled and sequenced on four lanes of the Illumina HiSeq 2000 platform (Illumina, USA) to generate paired-end reads. Symbiont-originated reads were found in the symbiotic gastrodermal samples; however, there were not enough reads to analyze the expression profile of the symbionts. The expression level of revised *Aiptasia* gene models [49, 50] was quantified using kallisto [51]. Differential expression analysis was performed using sleuth [52]. GO enrichment analysis was conducted on the differentially expressed genes using topGO [53], as described in Cui *et al.* [49]. It should be noted that KEGG pathway analysis in this study was based on mammalian and yeast genes due to the lack of KEGG pathway data for *Aiptasia*, so confirming whether the genes discovered in *Aiptasia* perform the same functions would require future work.

**2.1.3. Confirmation of Gene Identity.** Protein sequences of differentially expressed transcripts from the *Aiptasia* transcriptome were BLAST searched using the BLASTp function against the NCBI non-redundant database. Genes were annotated based on the hits with an *e* value above  $1 \times 10^{-5}$ . *Aiptasia* genes were then submitted to InterProScan [54] to identify gene domains and check that they matched to the gene annotation based on the NCBI non-redundant database results. Homologs from other eukaryotes were acquired and aligned against the *Aiptasia* genes using the MUSCLE alignment in Geneious v.11.1.5. Alignments were trimmed and run through ProtTest (v3.4.) [55] to find the optimal model of evolution using the corrected Akaike information criterion (AICc). Maximum-likelihood trees were then generated by PhyML (v3.1) [56], and branch support was calculated using aLRT analysis. aLRT has been shown to produce similar final tree topologies to bootstrap analysis [57, 58]. Trees were rooted for CDK and cyclin genes using sister genes from *Homo sapiens*, whilst all other trees were rooted using homologs from Placozoa, Porifera, or *Arabidopsis thaliana*. Trees were edited in the interactive tree of life (iTOL) software (v.5.6.3) [59]. The final classification of *Aiptasia* transcripts was based on these phylogenies.

**2.1.4. Data Accession.** The tissue-specific transcriptome method described in this current study and the cell-cycle transcript data collected are part of a wider transcriptome dataset collected by Cui *et al.* (in prep.). The full transcriptome dataset can be accessed at the NCBI database (accession number: PRJNA631577). The data for this specific study can be found in Supplementary File 1.

## 2.2. Microscopic Analysis of Host Cell Proliferation

**2.2.1. Modification of *Aiptasia* Symbiotic State.** In this study, clonal *Aiptasia* were used in three different symbiotic states: fully symbiotic, symbiont-free (i.e., aposymbiotic), and two days postinoculation with cultured symbionts. In total, 45 anemones were used in this study, with 15 animals per symbiotic state. These anemones were distributed across three 6-well plates, with three biological replicates *per well*. Experimental conditions were chosen to mimic field conditions as closely as possible, with animals kept at  $25^\circ\text{C}$  in autoclaved seawater from the Red Sea, with the salinity adjusted to  $\sim 37$  ppt. The irradiance was similar to that measured on local Red Sea reefs ( $\sim 40 \mu\text{mol photons m}^{-2}\cdot\text{s}^{-1}$ ), set to a 12 h light/12 h dark cycle. All animals were fed with freshly hatched *Artemia* sp. nauplii approximately three times a week, with a water change on the day after feeding. The last feeding occurred two days before EdU imaging, so that feeding did not affect the host cell proliferation rate [14]. Recently inoculated anemones were obtained by inoculating aposymbiotic individuals with laboratory-cultured *Brevium minutum* (previously known as *Symbiodinium* clade B strain SSB01) two days before sample processing, to represent an early symbiotic state. Note that, while *Aiptasia* regularly associates with *B. minutum* across the Indo-Pacific region [60], this strain was not sourced from the stock anemone cultured used here.

**2.2.2. Visualization of Cell Proliferation.** To observe cell proliferation in *Aiptasia* tissues, we measured the incorporation of a thymidine nucleotide substitute 5-ethynyl-2'-deoxyuridine (EdU) into the DNA (Click-iT® EdU Imaging Kit, Invitrogen). Animals were exposed to 10  $\mu$ M EdU (solvent DMSO) for 48 h [61, 62]. After incubation, an equal volume of 3.7% MgCl<sub>2</sub> solution was added to seawater and this mixture was used to anesthetize anemones for 30 min. To initiate fixation of the specimens, they were held in 4% paraformaldehyde at 4°C overnight. Fixation was followed by washing the specimens twice with phosphate buffer saline (PBS) and dehydration with ethanol. Dehydration was performed by transferring animals into 50%, 60%, 70%, 80%, and 95% EtOH for 10 min at each concentration. Following this incubation, animals were transferred into absolute EtOH twice for 15 min and then into m-Xylene twice for 15 min. Specimens were then embedded in paraffin and sectioned with a rotary microtome to a thickness of 7  $\mu$ m, and the sections were gently positioned on glass slides. A minimum of three slides were analyzed *per* individual. The paraffin was then carefully removed, and samples were rehydrated by placing them in m-Xylene for 15 min. After the m-Xylene incubation, the slides were transferred to 100%, 80%, 60%, and 50% EtOH and incubated for 7 min at each concentration. After rehydration, slides were washed once with PBS, and a blocking solution of 3% bovine serum albumin (BSA) in PBS was applied before permeabilizing the samples with 0.5% Triton X-100 in PBS. Additional washes with the blocking solution (3% BSA in PBS) and then with PBS were performed. Samples were treated with Click-iT® EdU reaction cocktail, prepared according to the manufacturer's recommendations, and incubated at room temperature for 30 min in the dark. A negative control, without Click-iT® reaction, was also imaged ( $n = 3-4$  *per* symbiotic state). After the 30 min incubation, the reaction mixture was washed with PBS, followed by Hoechst 33342 staining at a final concentration of 3  $\mu$ g/mL for 10 min in the dark to visualize all nuclear DNA. Slides were thoroughly washed once more with PBS and then mounted and imaged.

A Leica SP8 TCS STED 3 $\times$  confocal microscope was used to observe the EdU and Hoechst 33342 fluorescence signals. Images were taken where gastrodermal and epidermal tissues could be identified in up to three random areas. Acquired pictures were analyzed with CellProfiler 3.1.9 [63] using an adapted pipeline for particle counting from the manufacturer. Nuclei from both gastrodermal and epidermal tissue layers were counted together and separately (see below). Unfortunately, not every biological replicate produced good quality pictures, which led to some of the individuals not being used for further analysis. Altogether, 10 aposymbiotic individuals, 12 inoculated individuals, and 14 fully symbiotic individuals were analyzed for host cell proliferation counts.

**(1) Nuclei Counts.** Proliferating cell counts obtained from Click-iT® EdU-stained cells were normalized to the Hoechst 33342-stained nuclei number, as a proxy for the total cell number. Mean values of nuclei count *per* sample were calculated based on the counts from two to three images, depend-

ing on the image quality. Statistical analysis was performed using R version 3.5.2 [64]. The normality of the data distribution was determined with the Shapiro-Wilk test. Outlier values found in the datasets were removed from further analysis. Evaluation of homogeneity of variances was conducted using Levene's test, followed by a Student's *t*-test for independent samples to compare between different conditions. A *p* value < 0.05 was classed as statistically significant.

**(2) Nuclei Counts in Separate Tissue Layers.** To calculate the cell proliferation rate in separate tissue layers, fluorescence microscopy images were analyzed once more, this time by manually counting the nuclei using ImageJ software with the Cell Counter plugin [65]. We selected representative 150  $\mu$ m by 50  $\mu$ m areas within the gastrodermis and epidermis and separated different channels from the original picture into blue (for Hoechst 33342 signal) and green (for EdU signal). Five images were analyzed *per* symbiotic state (aposymbiotic, recently inoculated and symbiotic). The EdU nuclei count number was normalized to the total nuclei number (Hoechst 33342-stained nuclei). Statistical analysis was performed using R version 4.0.0 [64]. The normality of data distribution was determined with the Shapiro-Wilk test, while the homogeneity of variances was evaluated using Levene's test. Comparisons between groups were performed using the Student's *t*-test for independent samples and analysis of variance (ANOVA). Games-Howell *post hoc* analysis was used to further investigate significant differences after performing analysis of variance. A *p* value < 0.05 was considered to show statistically significant differences.

### 3. Results/Discussion

**3.1. Differentially Expressed Genes (DEGs) between Symbiotic States and Host Tissues.** Altogether, 29 transcripts differed in expression with regard to the symbiotic state and tissue type (Table 1). These transcripts corresponded phylogenetically to at least 25 separate *Aiptasia* cell-cycle genes (Supplementary Figures 1–22). Only one cell-cycle transcript was discarded after bioinformatic analysis (AIPGENE27523). This transcript was originally annotated as SMAD4, and when searching against the *Aiptasia* genome [48], the transcript also corresponded to a gene annotated as SMAD4. However, after BLAST searches against both the NCBI database and Reef Genomics database, analyzing the conserved domains, and subsequent phylogenetic analysis, it could not be determined whether the transcript was a SMAD protein or a myosin protein.

**3.1.1. Symbiotic Gastrodermis versus Aposymbiotic Gastrodermis.** The levels of 21 transcripts differed between the gastrodermis with and without symbionts. Eight transcripts showed elevated expression in the symbiotic gastrodermis when compared with the aposymbiotic gastrodermis (Table 1; Figure 1), and this mainly included genes involved in G<sub>0</sub> to G<sub>1</sub> phase transitions, whilst the remaining 13 transcripts which showed a depressed expression were mainly involved in DNA synthesis and mitosis.

TABLE 1: Differentially expressed host cell-cycle genes between symbiotic states and host tissues in Aiptasia. Numbers represent log-fold change in expression between samples.

Gene	Cell-cycle stage	Role	References	Aiptasia transcript ID	Symbiotic gastrodermis vs aposymbiotic gastrodermis	Symbiotic gastrodermis vs epidermis of symbiotic hosts	Epidermis of symbiotic vs aposymbiotic hosts	Aposymbiotic gastrodermis vs epidermis of aposymbiotic hosts
ATM/ATR	S	DNA damage response proteins that check for DNA damage during DNA replication; activation leads to apoptosis and cell-cycle arrest at the S and G <sub>2</sub> /M checkpoints and DNA repair	[41]; [66]	AIPG ENE9815		<b>-0.821</b>		
Bub1	G <sub>2</sub>	Forms the mitotic checkpoint complex (MCC); MCC produces the “wait anaphase” signal and inhibits the anaphase promoting complex APC/C by directly phosphorylating its activator (Cdc20) in the interphase, allowing the accumulation of cyclin B in the G <sub>2</sub> phase and inhibiting mitotic exit	[67]; [68]; [69]; [70]; [71]; [72]; [73]	AIPG ENE2130	<b>-0.833</b>			
Cdc14A phosphatase	M	Regulation of the G <sub>2</sub> /damage checkpoint and essential for the exit from mitosis by dephosphorylation of CDK1 substrates—mitotic cyclins; indirect role during DNA replication by suppressing CDKs upon mitotic exit, allowing the effective formation of pre-RC complexes during the S phase	[74]; [75]; [76]; [77]; [78]	AIPG ENE20570	<b>1.492</b>			<b>-0.584</b>
Cdc20	M	Activator of anaphase-promoting complex (APC/C) which initiates chromosome separation and subsequently destroys cyclin B and deactivates CDK1, allowing the exit from mitosis and the completion of the cell cycle	[79]; [70]	AIPG ENE561	<b>-1.489</b>			
Cdc25B,C	G <sub>2</sub> /M	Phosphorylation of Cdc25B activates the cyclin B-CDK1 complexes whose activity remains high until anaphase	[80]; [81]; [82]	AIPG ENE19331	<b>-1.022</b>			
Cyclin B	M	Forms complex with CDK1 in mitosis and required for mitotic progression	[83]	AIPG ENE10534	<b>-1.255</b>			

TABLE 1: Continued.

Gene	Cell-cycle stage	Role	References	Aiptasia transcript ID	Symbiotic gastrodermis vs aposymbiotic gastrodermis	Symbiotic gastrodermis vs epidermis of symbiotic hosts	Epidermis of symbiotic vs aposymbiotic hosts	Aposymbiotic gastrodermis vs epidermis of aposymbiotic hosts
CDK1	G <sub>2</sub> /M	Forms complex with cyclin A in the G <sub>2</sub> phase to fortify cells for commitment to mitosis as it is an upstream regulator of Plk1; forms complex with cyclin B in the M phase for mitotic progression	[84]	AIPG ENE3823	<b>-1.644</b>			
CDK4,6	G <sub>1</sub>	Regulator of the restriction point in G <sub>1</sub> through phosphorylation of the Rb-E2F complex	[85]	AIPG ENE14397	<b>-0.782</b>			
c-Myc	G <sub>0</sub>	Cell-cycle entry of quiescent (G <sub>0</sub> ) cells and increasing apoptotic sensitivity by amplifying death receptor pathways	[86]; [87]; [88]; [89]; [90]	AIPG ENE2563		<b>-3.550</b>		
				AIPG ENE2519		<b>-1.052</b>		
Dp-1,2	G <sub>1</sub> /S	Makes complexes with E2F transcription factors that then bind to different proteins and changes their function for cell-cycle progression	[91]	AIPG ENE10647	<b>1.356</b>			
				AIPG ENE22485	<b>1.439</b>	<b>1.881</b>		
				AIPG ENE22512	<b>-0.596</b>			
E2F1,2,3	G <sub>0</sub> to S	G <sub>0</sub> to S phase progression; DNA stability; transcriptional activators of essential cell-cycle genes	[91]	AIPG ENE28094			<b>1.287</b>	
GADD45	G <sub>2</sub> /M	Inhibitor of cyclin B/CDK1; apoptosis; cell-cycle arrest	[92]; [93]	AIPG ENE19027	<b>0.914</b>			
HDAC1	G <sub>1</sub> /S	Repress transcription through the deacetylation of lysine residues on histones, changing chromatin conformation and actively stopping protein function	[94]	AIPG ENE13245	<b>0.713</b>			
Mcm3		Forms MCM helicase complex that is required during DNA replication; loaded onto chromatin by the origin recognition complex (ORC) at the sites of replication during the G <sub>1</sub> phase; unwinds DNA; elicits replication and elongation; strict localization and timings to ensure that DNA replication only occurs once <i>per cell cycle</i>		AIPG ENE29020	<b>-0.675</b>	<b>-0.799</b>		
Mcm6	S		[95]; [96]; [97]; [98]	AIPG ENE8456	<b>-0.859</b>			

TABLE 1: Continued.

Gene	Cell-cycle stage	Role	References	Aiptasia transcript ID	Symbiotic gastrodermis vs aposymbiotic gastrodermis	Symbiotic gastrodermis vs epidermis of symbiotic hosts	Epidermis of symbiotic vs aposymbiotic hosts	Aposymbiotic gastrodermis vs epidermis of aposymbiotic hosts
Mdm2	G <sub>2</sub> /M	Antagonistic controller of p53 and inhibits its role in apoptotic initiation and the G <sub>1</sub> arrest; delays cell-cycle progression in the G <sub>2</sub> /M phase	[99]; [100]; [101]; [102]	AIPG ENE26697	<b>1.111</b>	<b>0.889</b>		
Mob1	M	Cell polarity marker involved in the mitotic exit network (MEN) signalling cascade and associates with spindle pole bodies throughout the cell cycle	[103]	AIPG ENE20640			<b>0.979</b>	
Mps1	M	Forms the mitotic checkpoint complex (MCC); MCC produces the “wait anaphase” signal and inhibits the anaphase promoting complex APC/C by directly phosphorylating its activator (Cdc20) in the interphase, allowing the accumulation of cyclin B in the G <sub>2</sub> phase and inhibiting mitotic exit	[67]; [68]; [69]; [70]; [71]; [72]; [73]	AIPG ENE12491	<b>-0.920</b>			
ORC3	S	Forms the ORC (origin recognition complex) and binds to replicating sequences in the chromatin, allowing the attachment of other replication proteins, e.g., MCM-helicase	[104]; [96]; [105]	AIPG ENE5780				<b>-0.675</b>
Plk1	M	Promotes mitotic entry by inducing the phosphorylation of Cdc25B/C and is the kinase required for mitotic spindle function in chromosome separation	[106]; [84]	AIPG ENE7783 AIPG ENE16487	<b>-0.583</b>	<b>-2.327</b>		
p27 kip1	G <sub>1</sub> /S	CDK inhibitor that binds to CDK 2-cyclin E complexes at the G <sub>1</sub> /S phase to inhibit cell-cycle progression	[107]; [108]	AIPG ENE22427				<b>-0.770</b>
SCF (Skp1/Cullin/F-Box protein)	G <sub>1</sub> /S	E3 ubiquitin ligase involved in controlling the progression of the cell cycle by degrading cell-cycle antagonists, e.g., p57, p27, p21, Wee1, and Emi1; regulates entry into the S phase with increasing levels destroying S-phase	[109]; [110]; [111]; [112]	AIPG ENE5823 (Cullin-1) AIPG ENE15738 (S-phase associated kinase)	<b>0.504</b> <b>1.180</b>			<b>-0.902</b>

TABLE 1: Continued.

Gene	Cell-cycle stage	Role	References	Aiptasia transcript ID	Symbiotic gastrodermis vs aposymbiotic gastrodermis	Symbiotic gastrodermis vs epidermis of symbiotic hosts	Epidermis of symbiotic vs aposymbiotic hosts	Aposymbiotic gastrodermis vs epidermis of aposymbiotic hosts
		antagonists p21 and p27, allowing the cells to enter the S phase		AIPG ENE15719 (S-phase associated kinase)				
14-3-3 protein	G <sub>2</sub> /M	Regulates Cdc25B/C	[80]	AIPG ENE804	-0.479			

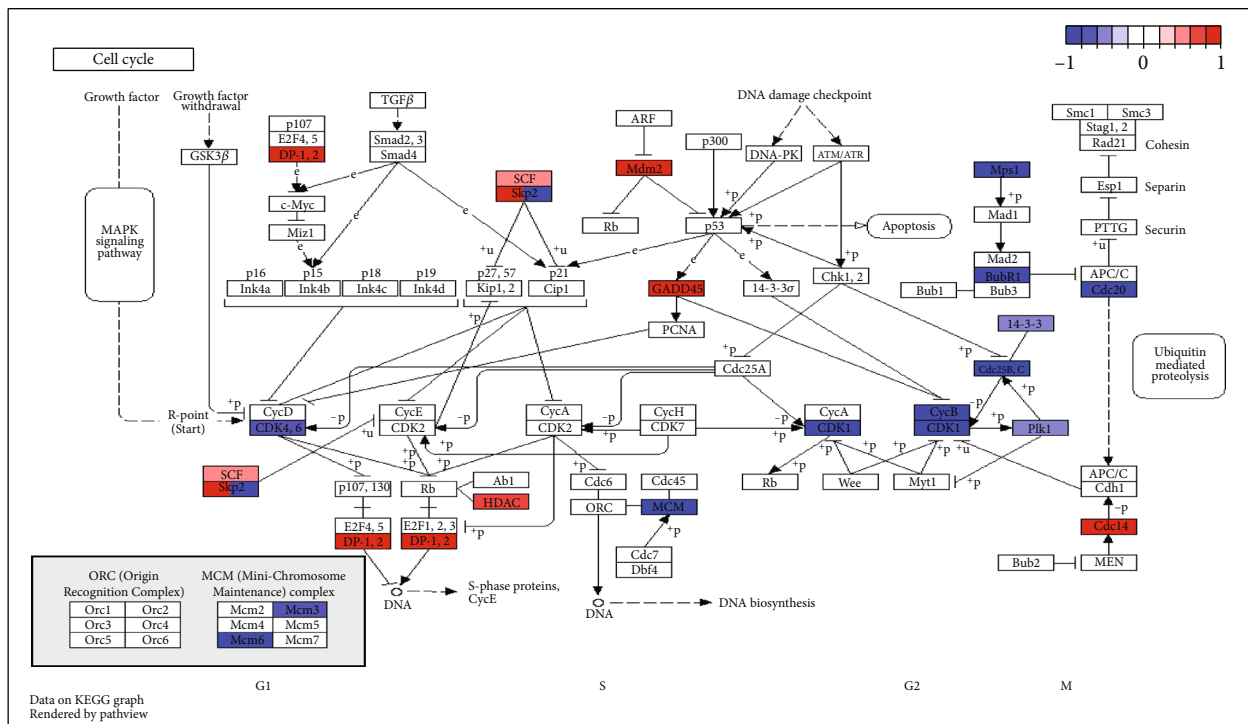


FIGURE 1: KEGG map of differentially expressed host cell-cycle genes between the symbiotic gastrodermis when compared with the aposymbiotic gastrodermis. Scale represents the fold-change in expression. Blue signifies downregulation and red signifies upregulation.

These results suggest that the presence of symbionts in the gastrodermis may arrest more host cells at the G<sub>1</sub>/S-phase checkpoint than in aposymbiotic hosts, and subsequently inhibit the mitotic progression and completion of a larger proportion of host cells (Figure 2).

(1) *G<sub>1</sub>-Phase Genes.* Cullin-1 and an S-phase-associated kinase that form part of the SCF (Skp1-Cul1-F-box protein) were upregulated in the symbiotic gastrodermis. SCF and APC/C (anaphase-promoting complex or cyclosome) are the two major E3 ubiquitin ligases involved in controlling the cell cycle [112]. SCF acts throughout the cell cycle and regulates entry into the S phase by degrading cell-cycle

antagonists that inhibit cell-cycle progression (Table 1; [110, 111]). It is unclear whether the SCF was promoted or inhibited in the symbiotic gastrodermis when compared with the aposymbiotic gastrodermis as, although a cullin-1 transcript and a S-phase kinase transcript were elevated, another S-phase kinase transcript (AIPGENE15719) showed a decrease in expression.

CDK4/6 was downregulated in the symbiotic gastrodermis. CDK4/6 is active in the G<sub>1</sub> phase, and its function is to phosphorylate the Rb-E2F complex at the restriction checkpoint in the G<sub>1</sub>/S phase [85]. Until phosphorylation by CDK4/6, the Rb-E2F complex represses the transcription



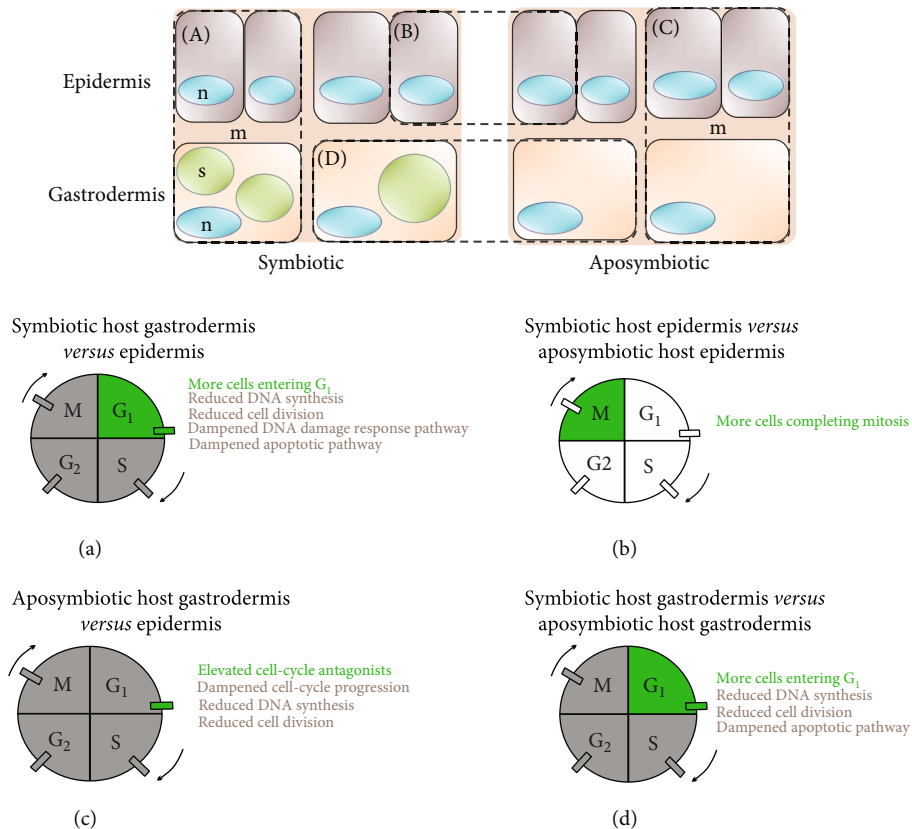


FIGURE 2: Differences in host cell-cycle gene expression and progression between symbiotic states and tissue types in Aiptasia. Green symbolizes upregulated and grey represents downregulated cell-cycle phases, whilst white represents no recorded changes to the cell-cycle phase in the respective comparisons. “s” refers to symbiont, “n” refers to host nuclei, and “m” refers to mesoglea.

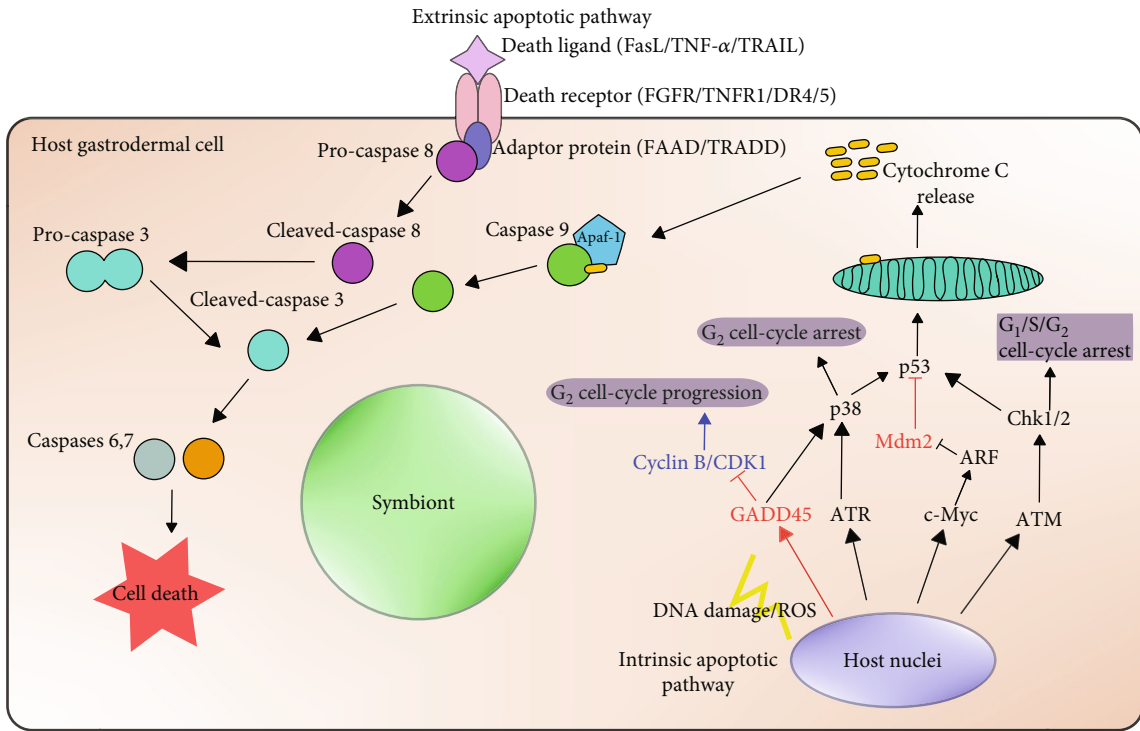
factor complex, E2F-Dp, by histone deacetylase (HDAC) activity [113–116]. This gene suppression negatively regulates the  $G_1/S$  transition [117]. As HDACs were upregulated in the symbiotic gastrodermis and CDK4/6 was downregulated, it suggests that HDACs were inducing the arrest of the gastrodermal cells at the restriction point in the  $G_1$  phase.

Two out of three Dp-1,2 transcripts showed elevated expression in the symbiotic gastrodermis, whilst the third showed a decrease in expression. Dp proteins form complexes with transcription factor E2F [118]. There are two types of E2F which have different functions: E2F1-3 are transcriptional activators whereas E2F4-5 are transcriptional suppressors [118]. As it is unknown which Dp transcripts were associated with transcriptional suppressors (E2F4-5) or activators (E2F1-3), it is hard to draw conclusions about what this finding may mean. However, as genes involved in transcriptional suppression were upregulated (HDAC) and genes involved in  $G_1$  progression were downregulated (CDK4/6), it is fair to assume that the upregulated Dp gene transcripts do not lead to cell-cycle progression.

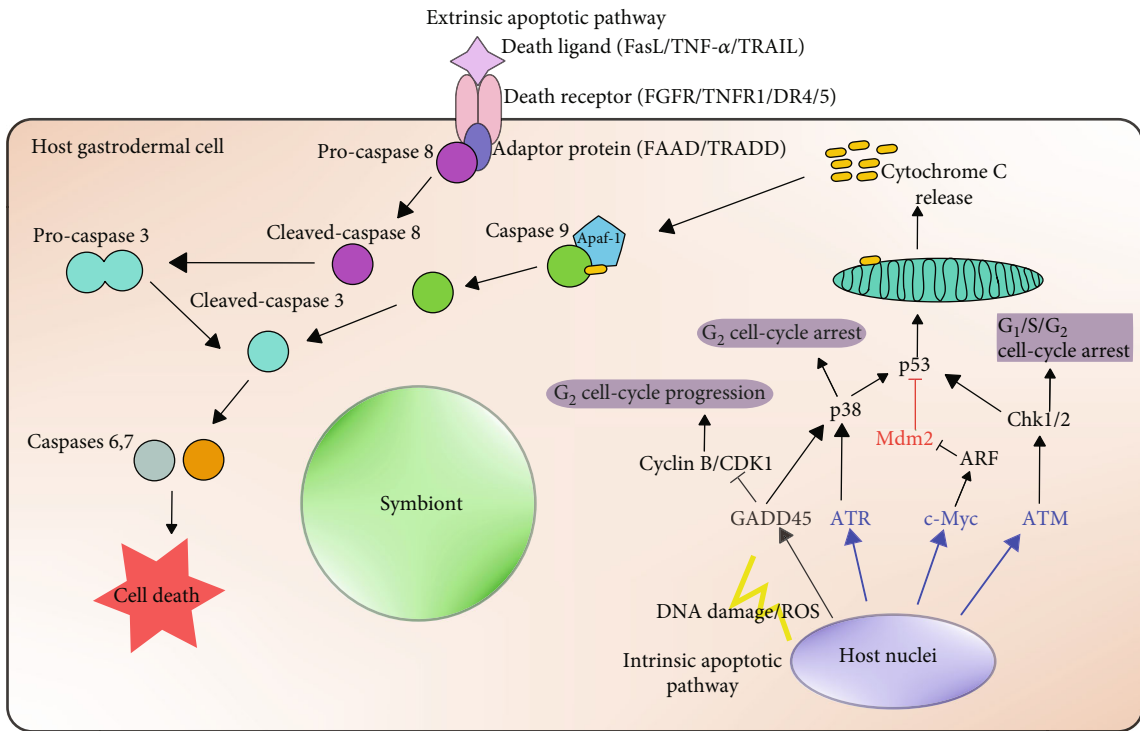
**(2) S-Phase Genes.** Two important genes involved in DNA synthesis were downregulated in the symbiotic gastrodermis: Mcm3 and Mcm6. The mini-chromosome maintenance proteins (Mcm2-7) are essential for the initiation of DNA replication during the S phase, as their function

is to identify chromatin which can duplicate in the  $G_2/M$  phase [97]. Mcm3 inhibition leads to the arrest of cells in  $G_1$  with unduplicated DNA [119]. Thus, the downregulation of Mcm3 and Mcm6 suggests that, in the presence of symbionts, fewer gastrodermal host cells synthesize DNA. This may be a regulatory path elicited by the presence of the symbiont to allow algal proliferation while slowing the proliferation of host cells. This has been shown to occur in certain viral infections, where the downregulation of the host’s prereplication complex facilitates proliferation of the viral infection [120].

**(3)  $G_2/M$ -Phase Genes.** Two antagonists of the cyclin B-CDK1 complex were simultaneously upregulated in the symbiotic gastrodermis—GADD45 and Cdc14 (Table 1)—whilst many genes involved in mitotic progression were downregulated (Figure 1). GADD45 is a potent inhibitor of the CDK1/cyclin B complex [92, 93] and is a protein often induced by cellular stress, such as DNA damage, cell injury, apoptosis, and cell-cycle checkpoint maintenance in growth arrest [93] (Figure 3(a)). In addition to inhibiting the CDK1/cyclin B complex, GADD45 can block the activator of this complex, Cdc25B/C [81]. The upregulation of GADD45 may therefore explain the downregulation of CDK1, cyclin B (and presumably the CDK1/cyclin B complex), Cdc25B/C, and the regulator of Cdc25B/C, 14-3-3, in the symbiotic gastrodermis.



(a) Symbiotic gastrodermis versus aposymbiotic gastrodermis



(b) Symbiotic gastrodermis versus epidermis of symbiotic hosts

FIGURE 3: Apoptosis pathway changes in the host elicited by the presence of the symbiont in the gastrodermal tissue. Red text and arrows refer to upregulated genes and blue text and arrows refer to downregulated genes.

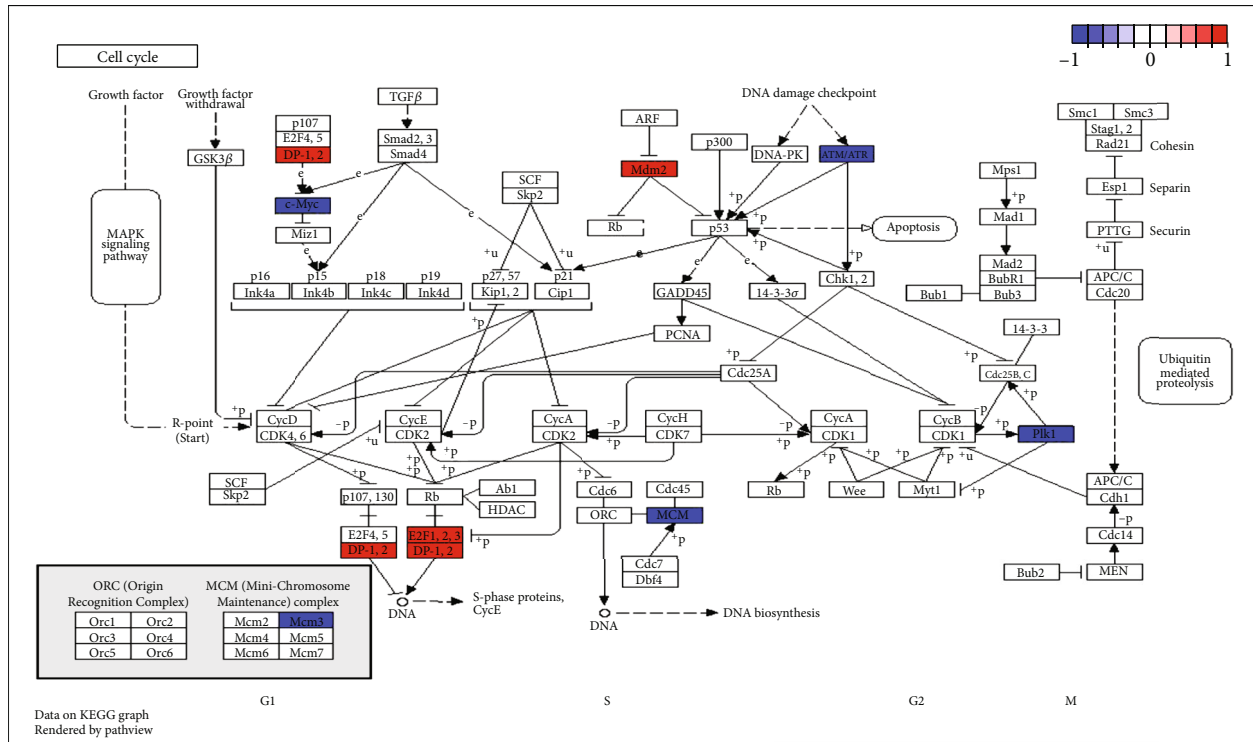


FIGURE 4: Differences in host cell-cycle gene expression in the symbiotic gastrodermis when compared with the epidermis of symbiotic anemones. The scale represents the fold-change in expression. Blue signifies downregulation and red signifies upregulation.

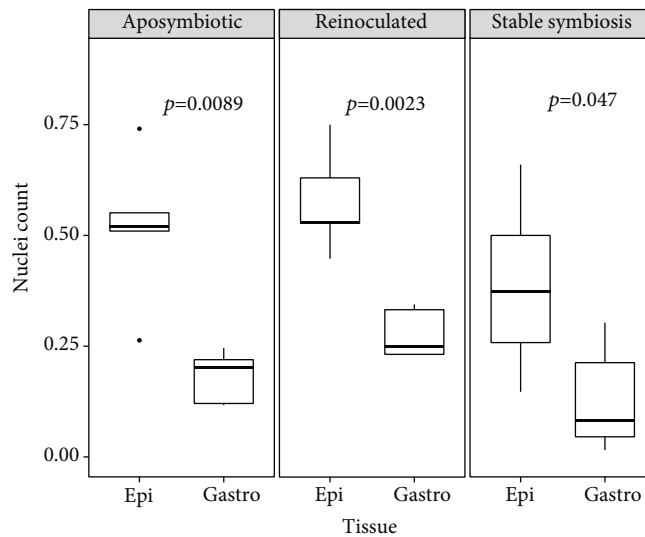


FIGURE 5: Cell proliferation rate comparisons between the epidermal and gastrodermal tissues of different symbiotic-state animals. Ratios were calculated *via* quantifying the number of Hoechst- and EdU-stained nuclei in microscope images ( $n = 5$ ) in each tissue layer separately. Statistical significance of pairwise comparisons between the different tissue layers was calculated using a Student's *t*-test and is represented by the *p* value in the graphs. Epi: epidermal tissue layer; Gastro: gastrodermal tissue layer.

As CDK1 was downregulated in the symbiotic gastrodermis and it is the upstream regulator of the mitotic cascade (through activating the gene required for mitotic entry, Plk1, during its association with cyclin A) [84], this may explain the subsequent downregulation of downstream mitotic progression genes (Bub1, Plk1, Mps1, Cdc20, and cyclin B; Table 1).

GADD45 can also induce an apoptotic cascade by p38 activation, which in turn activates the tumour suppressor gene p53 and creates a positive feedback loop ([93]; Figure 3(a)). However, p53 expression remained unchanged, and instead, we saw its antagonistic controller Mdm2 upregulated (Table 1). This suggests that the end point of the GADD45 upregulation was likely to be the downregulation

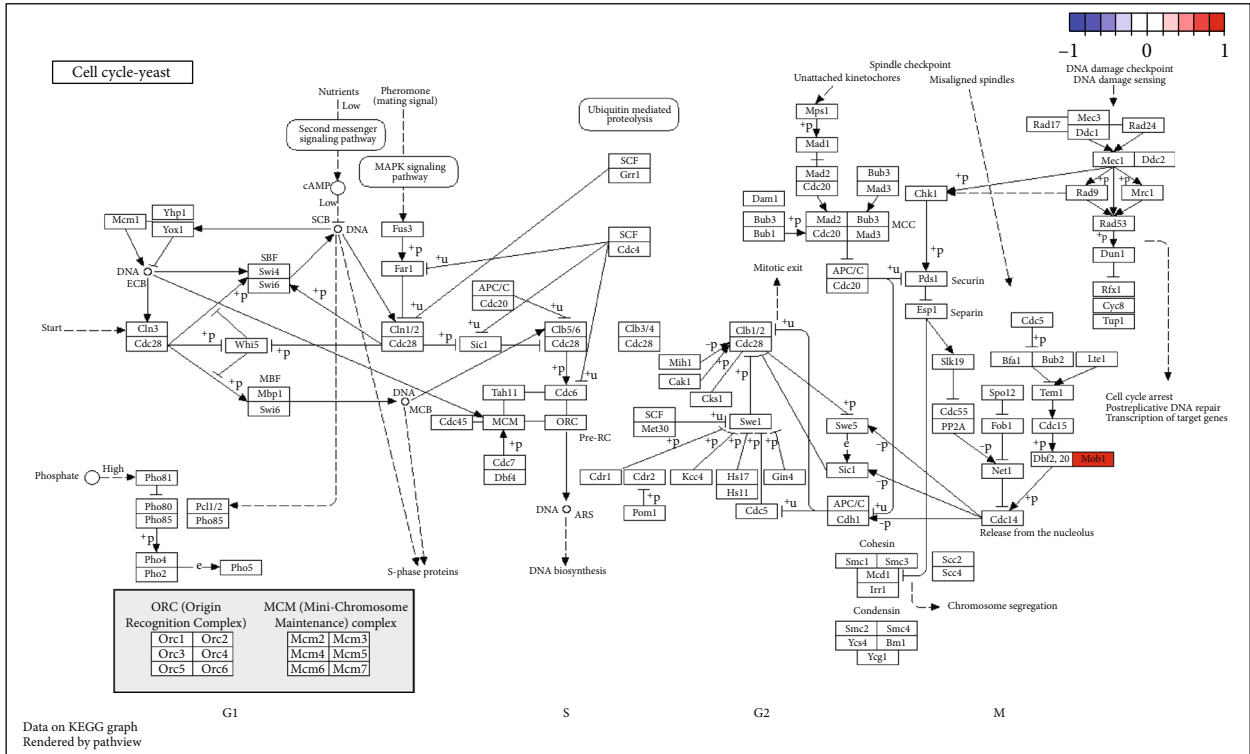


FIGURE 6: Differences in host cell-cycle gene expression in the epidermis of symbiotic anemones compared with aposymbiotic anemones. The scale represents the fold change in expression. Blue signifies downregulation and red signifies upregulation.

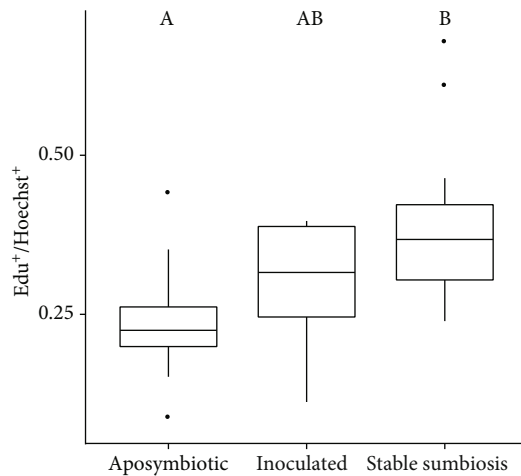


FIGURE 7: Cell proliferation rates calculated as the proportion of Hoechst-positive to EdU-positive cells in aposymbiotic ( $n = 10$ ), recently inoculated ( $n = 12$ ), and fully symbiotic ( $n = 14$ ) hosts. Ratios were calculated *via* quantifying the number of Hoechst- and EdU-stained nuclei in microscope images ( $n = 2 - 3$  per host) where gastrodermal and epidermal tissues could be identified. Statistical significance of pairwise comparisons was calculated using a Student's *t*-test and is indicated by letters above the boxplots. Statistical significance of difference among the three groups was calculated by one-way ANOVA,  $p = 0.013$ .

of the cyclin B-CDK1 complex rather than p53 activation (Figure 3(a)). This finding agrees with a past study investigating gene expression changes caused by the symbiotic state in *Aiptasia* [36] that found that symbiosis elicited the upregulation of GADD45 by 5.1-fold. Furthermore, the same study identified the apoptotic pathway as one of the main cellular functions that differed between symbiotic states,

with 13 genes significantly changing their expression [36]. The upregulation of *Mdm2* suggests that the presence of compatible symbionts reduces apoptotic rates in host cells, agreeing with a past study [37], which found decreases in host apoptosis in the presence of homologous symbionts compared with aposymbiotic anemones under stable conditions.

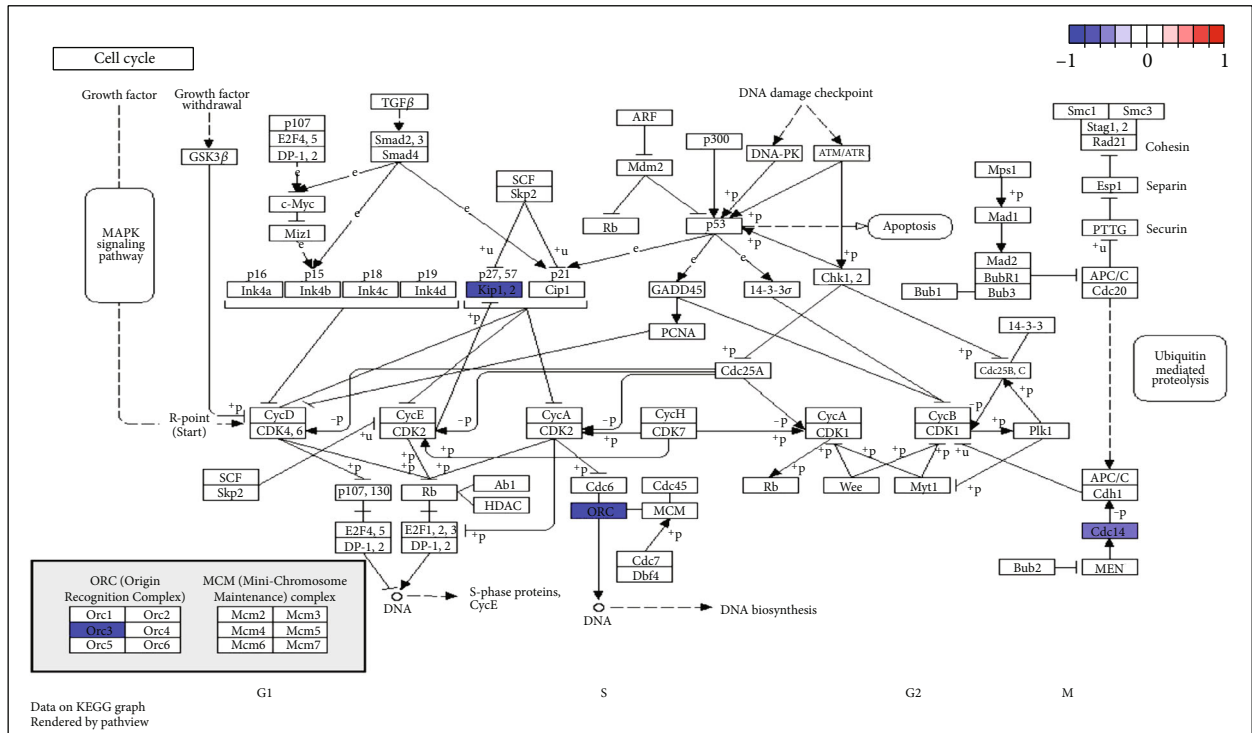


FIGURE 8: Differences in host cell-cycle gene expression in the gastrodermis when compared with the epidermis of aposymbiotic anemones. The scale represents the fold change in expression. Blue signifies downregulation and red signifies upregulation.

A triggering of an apoptotic cascade by the host in the presence of symbionts is consistent with this post-phagocytotic mechanism controlling the symbiont population, as had been suggested previously with respect to symbiosis onset, and homeostatic and stress-induced regulation of the symbiont population in the fully symbiotic state [4, 18, 25]. Therefore, it favours the symbiont to block host apoptotic mechanisms to allow persistence within the host. Along with apoptosis regulation, Mdm2 also delays cell-cycle progression through the G<sub>2</sub>/M phase by degrading Cdc25C [121]. Thus, both the upregulation of Mdm2 and the downregulation of genes that facilitate G<sub>2</sub>/M progression highlight the reduction of host gastrodermal cells progressing through, and completing, mitosis in the presence of symbionts.

**3.1.2. Differentially Expressed Genes (DEGs) in the Symbiotic Gastrodermis versus Epidermis of Symbiotic Anemones.** In the current study, three genes were differentially upregulated, Dp-1,2, Mdm2, and E2F1-3, while four were downregulated, ATM/ATR, PIK1, Mcm3, and c-Myc, in the gastrodermis versus epidermis of symbiotic anemones (Figure 4).

**(1) G<sub>1</sub>/S-Phase Genes.** Dp-1,2 levels were upregulated in the symbiotic gastrodermis versus the epidermis of symbiotic anemones as with the symbiotic gastrodermis versus aposymbiotic gastrodermis. The partners of Dp-1,2, E2F1-3, were also upregulated. These complexes have cyclical interactions with important regulators of the cell cycle, e.g., cyclin A [91, 122]. The upregulation of the transcriptional activator E2F-

Dp complex points to increased numbers of cells transcribing genes for cell-cycle progression in the G<sub>1</sub>/S-phase transition [123], compared with epidermal cells (Figure 2).

However, although more cells were transcribing genes for cell-cycle progression in the G<sub>1</sub>/S phase, genes essential for DNA replication (Mcm3) were downregulated in the gastrodermis versus epidermis of symbiotic anemones. This suggests that the presence of symbionts elicits increased transcription of cell-cycle genes but reduced DNA synthesis in host gastrodermal cells, as confirmed here via fluorescence microscopy (Figure 5).

Genes with functions in apoptotic initiation (e.g., DNA damage response proteins ATM/ATR and the apoptotic sensitizer c-Myc) were downregulated in the symbiotic gastrodermis relative to the epidermis of symbiotic anemones (Table 1; Figure 3(b)). In cnidarians, apoptosis has been shown to influence the colonization success of symbionts in a host, with high levels of apoptosis reducing colonization success [18]. Likewise, host apoptosis has been shown to increase and contribute to the loss of the resident symbiont population under stress, i.e., bleaching [17, 124]. Furthermore, previous studies have shown that host apoptotic gene expression decreases in the presence of symbionts [37] and that the inhibition of host apoptosis allows the recolonization of hosts by symbionts during thermal stress [124]. Altogether these findings, along with the findings in this current study, suggest that host apoptosis is a major regulatory mechanism of the symbiont population that is influenced by both the host's symbiotic state and stress.

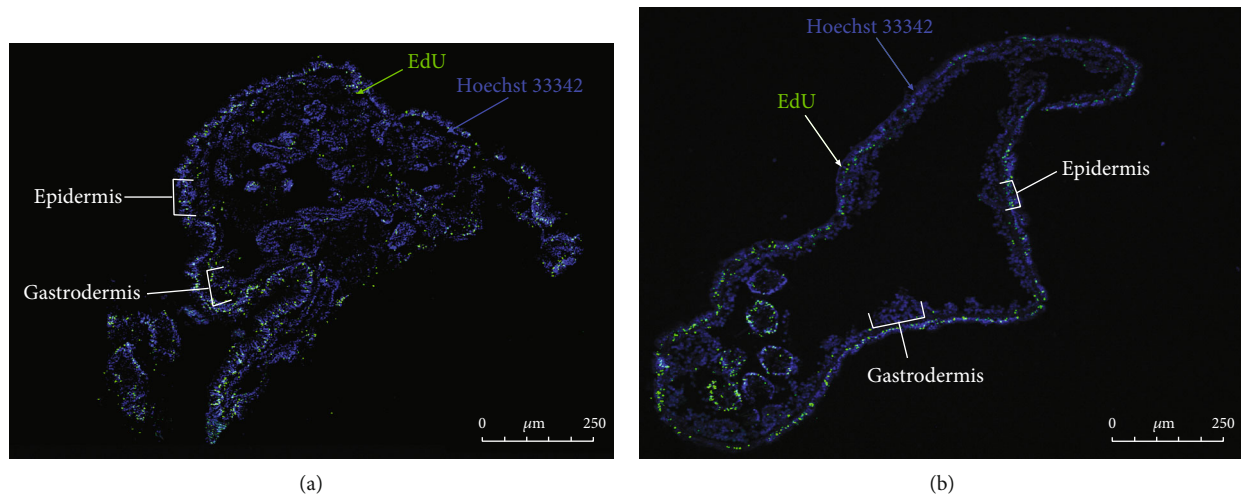


FIGURE 9: Transverse section of an aposymbiotic Aiptasia column (a) and a symbiotic Aiptasia column (b). Sections are stained with Hoechst 33342 (blue) and EdU (green), visualized under a fluorescence microscope. Blue cells indicate all noncycling Aiptasia cells present, whereas green cells indicate the proliferating (cycling) Aiptasia cells, through the incorporation of EdU into cells progressing through their cell cycle during DNA synthesis (S phase).

(2) *G<sub>2</sub>/M-Phase Genes*. Mdm2, the antagonistic controller of p53 and the G<sub>2</sub>/M phase inhibitor, was upregulated in the symbiotic gastrodermis when compared with the epidermis in the symbiotic state, as well as the aposymbiotic gastrodermis (Table 1; Figure 3(b)). Furthermore, Plk1, required for mitotic spindle assembly (Table 1; [84]), was also downregulated. This further suggests that there is a downregulation in the host apoptotic pathway and fewer cells progressing through mitosis in the symbiotic gastrodermis.

ATM/ATR was downregulated in the symbiotic gastrodermis *versus* the epidermis of symbiotic anemones. ATM and ATR are two of the three kinases (the other being DNA-PK) that control the DNA damage response (DDR) pathway in cells [66]. The downregulation of ATM/ATR may be another method employed by the symbiont to allow its persistence and proliferation. Viruses have been shown to inhibit ATM/ATR, as viral proliferation induces the DDR pathway which would limit the proliferation of the infection through upregulating cell checkpoint pathways [66, 125]. Interestingly, ROS have also been shown to induce ATM activation [126]. Thus, it would be interesting to know whether the symbiont reduces the host's sensitivity to ROS by downregulating ATM/ATR, with ROS being a known driver for coral bleaching and the subsequent expulsion of symbionts [127]. This hypothesis warrants future investigation.

**3.1.3. Differentially Expressed Genes (DEGs) in the Epidermis of Symbiotic Anemones versus the Epidermis of Aposymbiotic Anemones.** Only one gene was differentially expressed in the epidermis of symbiotic *versus* aposymbiotic anemones: Mob1 (Table 1; Figure 6). The upregulation of the protein required for mitotic exit, Mob1, may highlight that more host cells are exiting mitosis in the epidermis when in the symbiotic state (Figure 2). This finding agrees with both the cell proliferation rates found in the current study

(Figure 7), which revealed that host cell proliferation was lowest in aposymbiotic anemones, and findings from a previous study which showed that host cell division was upregulated in the presence of symbionts [27].

It is well known that symbiotic algae translocate photosynthetic products to their cnidarian hosts, supporting the host's metabolism, growth, and reproduction [128, 129]. Consequently, growth rates in symbiotic hosts are higher than those in aposymbiotic ones, even with host feeding [130, 131], with enhanced growth presumably occurring in all tissues irrespective of whether symbionts are present or not [27].

**3.1.4. Differentially Expressed Genes (DEGs) of the Gastrodermis versus Epidermis of Aposymbiotic Anemones.** In the aposymbiotic state, only three genes were differentially expressed in the gastrodermis versus the epidermis: p27<sup>kip1</sup>, ORC3, and Cdc14 (Table 1; Figure 8). All three DEGs in the aposymbiotic gastrodermis were downregulated; however, p27<sup>kip1</sup> is a cell-cycle antagonist, while ORC3 and Cdc14 are cell-cycle synergists (Table 1).

The downregulation of all cell-cycle genes in the aposymbiotic gastrodermis compared with the epidermis of aposymbiotic anemones suggests that, as in the symbiotic state, fewer gastrodermal than epidermal cells were progressing through the cell cycle (Figure 2). This highlights that the epidermis has a higher host-cell turnover regardless of the symbiotic state, agreeing with past studies [27, 61, 132, 133].

**3.2. Cell Proliferation in Different Symbiotic States.** Following the findings of the transcriptomic analysis, host-cell proliferation of Aiptasia in different symbiotic states was measured to determine whether the presence of symbionts did indeed cause an increase in cell turnover. Microscopic analysis revealed that the EdU nucleotide was successfully incorporated into both gastrodermal and epidermal cells of all animals, irrespective of the symbiotic state (Figure 9). Samples

that were not treated with the Click-iT® EdU reaction mix showed no EdU signal (data not shown), confirming EdU incorporation specificity and the absence of significant auto-fluorescence from tissues.

When the gastrodermal and epidermal tissue layers were analyzed together, the presence of symbionts significantly changed the proliferation rate of host cells (one-way ANOVA,  $F(2, 32) = 5.295$ ,  $p = 0.01$ ), with fully symbiotic anemones having a significantly higher host-cell proliferation rate ( $0.39 \pm 0.04$  Edu<sup>+</sup>/Hoechst<sup>+</sup> cells) than aposymbiotic anemones ( $0.24 \pm 0.03$  Edu<sup>+</sup>/Hoechst<sup>+</sup> cells) (Tukey *post hoc*,  $p = 0.008$ ; Figure 7). However, there was no statistical difference between recently colonized Aiptasia and aposymbiotic anemones (Tukey *post hoc*,  $p = 0.388$ ). The similarity between recently colonized and aposymbiotic Aiptasia is possibly due to the low population density of symbionts in the former, with a concomitantly small amount of photosynthate translocated to the host and hence minimal influence on host cell growth.

When microscope imaging, it appeared that the epidermis had a greater number of proliferating cells than the gastrodermis in all symbiotic states (Figure 9). This was confirmed by additional image analysis, where we manually counted the nuclei of the epidermal and gastrodermal layers separately (Figure 5). There was a significantly higher number of proliferating host cells in the epidermis *versus* the gastrodermis in all symbiotic states (Student's *t*-test,  $p < 0.05$ ; Figure 5). This finding is consistent with the results from the DEG analysis and suggests that a smaller proportion of gastrodermal cells was progressing through mitosis (Table 1; Figures 2 and 4). Moreover, this finding agrees with a recent study that investigated the proliferation rate of host cells during symbiont colonization in Aiptasia [27]; these authors reported a proliferation rate of 58.3% *versus* 41.7% in the epidermis and gastrodermis, respectively. Similarly, in adult corals, the epidermis has been shown to have a faster proliferation rate in the symbiotic state than the gastrodermis [132]. Future work should aim at further confirming the nutritional benefit of symbionts to the host by investigating the effect of photosynthetic inhibitors on tissue-specific cell proliferation rates in the host in different symbiotic states.

#### 4. Conclusion

In summary, the presence of symbionts in gastrodermal cells is associated with (1) a downregulation of host apoptotic initiators and sensitizers, (2) the downregulation of genes that function in G<sub>1</sub> and mitotic progression, (3) the downregulation of genes involved in the DNA damage response pathway, and (4) the downregulation of genes involved in DNA synthesis, when compared with both aposymbiotic gastrodermal cells and epidermal cells in symbiotic hosts. The changes in host cell-cycle gene expression are likely to reflect the downstream pathways influenced by inter-partner communication during symbiosis and its subsequent regulation of the symbiont population, aiding the persistence and proliferation of this symbiont population in the host. In contrast to reduced mitotic progression and DNA synthesis in gastrodermal cells, our observations in the epidermal cells of

symbiotic anemones suggest that the presence of symbionts in the gastrodermis increases the rates of mitotic completion and host cell proliferation, possibly due to the translocation of photosynthetic products from the symbionts to the host. Our findings suggest which host genes play a role in symbiont persistence in the host cell and which genes are involved in host-cell proliferation in the symbiotic state, thereby furthering our understanding of host-symbiont biomass coordination in the cnidarian-dinoflagellate symbiosis.

#### Data Availability

Data associated with this manuscript is available in the supplementary files, and the full transcriptome dataset can be accessed at the NCBI database (accession number: PRJNA631577) (as stated in the Section 2.1.4 Data Accession).

#### Conflicts of Interest

The authors declare no competing interests.

#### Authors' Contributions

LMG wrote the manuscript, analyzed the transcriptomic data, and constructed Figures 2 and 3, as well as Table 1. MKK and GC collected the transcriptomic and microscopy data. MKK and GC also analyzed the microscope data and produced Figures 1 and 4–9. CAO, ARG, VMW, MA, and SKD helped edit the manuscript. All authors reviewed the manuscript before submission. Lucy M. Gorman and Migle K. Konciute are the co-first authors.

#### Acknowledgments

This research was supported by the Marsden Fund of the Royal Society Te Apārangi of New Zealand (grant number VUW1601), awarded to SKD, ARG, VMW, and CAO, and baseline funding from KAUST to MA.

#### Supplementary Materials

*Supplementary 1.* Supplementary File 1: Differences in expression of Aiptasia cell-cycle genes between the tissue type (gastrodermis *versus* epidermis) and symbiotic state (symbiotic *versus* aposymbiotic).

*Supplementary 2.* Figure S1-S22: Phylogenetic trees of differentially expressed Aiptasia cell-cycle genes detected between the symbiotic state and the tissue type. Colour of branches corresponds to aLRT support (SH-value). Aiptasia genes are written in blue. The phylogenetic trees were made using PhyML (v3.1) [54] and visualized using the Interactive Tree of Life software (v5.6.3) [57].

#### References

- [1] C. Parmesan, "Ecological and evolutionary responses to recent climate change," *Annual Review of Ecology, Evolution, and Systematics*, vol. 37, no. 1, pp. 637–669, 2006.

- [2] O. Hoegh-Guldberg, P. J. Mumby, A. J. Hooten et al., "Coral reefs under rapid climate change and ocean acidification," *Science*, vol. 318, no. 5857, pp. 1737–1742, 2007.
- [3] T. P. Hughes, A. H. Baird, D. R. Bellwood et al., "Climate change, human impacts, and the resilience of coral reefs," *Science*, vol. 301, no. 5635, pp. 929–933, 2003.
- [4] S. K. Davy, D. Allemand, and V. M. Weis, "Cell biology of cnidarian-dinoflagellate symbiosis," *Microbiology and Molecular Biology Reviews*, vol. 76, no. 2, pp. 229–261, 2012.
- [5] T. S. Wakefield, M. A. Farmer, and S. C. Kempf, "Revised description of the fine structure of in situ zooxanthellae genus *Symbiodinium*," *The Biological Bulletin*, vol. 199, no. 1, pp. 76–84, 2000.
- [6] T. S. Wakefield and S. C. Kempf, "Development of host- and symbiont-specific monoclonal antibodies and confirmation of the origin of the symbiosome membrane in a Cnidarian-Dinoflagellate symbiosis," *The Biological Bulletin*, vol. 200, no. 2, pp. 127–143, 2001.
- [7] C. Kopp, I. Domart-Coulon, S. Escrig, B. M. Humbel, M. Hignette, and A. Meibom, "Subcellular investigation of photosynthesis-driven carbon assimilation in the symbiotic reef *Coral Pocillopora damicornis*," *American Society for Microbiology*, vol. 6, no. 1, p. e02299, 2015.
- [8] M. S. Burriesci, T. K. Raab, and J. R. Pringle, "Evidence that glucose is the major transferred metabolite in dinoflagellate-cnidarian symbiosis," *Journal of Experimental Biology*, vol. 215, no. 19, pp. 3467–3477, 2012.
- [9] K. E. Hillyer, S. Tumanov, S. Villas-Bôas, and S. K. Davy, "Metabolite profiling of symbiont and host during thermal stress and bleaching in a model cnidarian-dinoflagellate symbiosis," *Journal of Experimental Biology*, vol. 219, no. 4, pp. 516–527, 2016.
- [10] L. Muscatine and C. Hand, "Direct evidence for the transfer of materials from symbiotic algae to the tissues of a coelenterate," *Proceedings of the National Academy of Sciences*, vol. 44, no. 12, pp. 1259–1263, 1958.
- [11] N. Rädcker, C. Pogoreutz, C. R. Voolstra, J. Wiedenmann, and C. Wild, "Nitrogen cycling in corals: the key to understanding holobiont functioning," *Trends in Microbiology*, vol. 23, no. 8, pp. 490–497, 2015.
- [12] M. S. Roth, "The engine of the reef: photobiology of the coral-algal symbiosis," *Frontiers in Microbiology*, vol. 5, p. 422, 2014.
- [13] R. J. Jones, "Zooxanthellae loss as a bioassay for assessing stress in corals," *Marine Ecology Progress Series*, vol. 149, pp. 163–171, 1997.
- [14] G. J. Smith and L. Muscatine, "Cell cycle of symbiotic dinoflagellates: variation in G<sub>1</sub> phase-duration with anemone nutritional status and macronutrient supply in the *Aiptasia pulchella*-*Symbiodinium pulchrum* symbiosis," *Marine Biology*, vol. 134, no. 3, pp. 405–418, 1999.
- [15] A. ClercqDe and D. Inzé, "Cyclin-dependent kinase inhibitors in yeast, animals, and plants: a functional comparison," *Critical Reviews in Biochemistry and Molecular Biology*, vol. 41, no. 5, pp. 293–313, 2006.
- [16] M.-C. Chen, M.-C. Hong, Y.-S. Huang, M.-C. Liu, Y.-M. Cheng, and L.-S. Fang, "ApRab11, a cnidarian homologue of the recycling regulatory protein Rab11, is involved in the establishment and maintenance of the *Aiptasia*-*Symbiodinium* endosymbiosis," *Biochemical and Biophysical Research Communications*, vol. 338, no. 3, pp. 1607–1616, 2005.
- [17] S. R. Dunn, C. E. Schnitzler, and V. M. Weis, "Apoptosis and autophagy as mechanisms of dinoflagellate symbiont release during cnidarian bleaching: every which way you lose," *Proceedings of the Royal Society of London B: Biological Sciences*, vol. 274, no. 1629, pp. 3079–3085, 2007.
- [18] S. R. Dunn and V. M. Weis, "Apoptosis as a post-phagocytic winnowing mechanism in a coral-dinoflagellate mutualism," *Environmental Microbiology*, vol. 11, no. 1, pp. 268–276, 2009.
- [19] R. D. Gates, G. Baghdasarian, and L. Muscatine, "Temperature stress causes host cell detachment in symbiotic cnidarians: implications for coral bleaching," *The Biological Bulletin*, vol. 182, no. 3, pp. 324–332, 1992.
- [20] G. Baghdasarian and L. Muscatine, "Preferential expulsion of dividing algal cells as a mechanism for regulating algal-cnidarian symbiosis," *The Biological Bulletin*, vol. 199, no. 3, pp. 278–286, 2000.
- [21] J. Dimond and E. Carrington, "Symbiosis regulation in a facultatively symbiotic temperate coral: zooxanthellae division and expulsion," *Coral Reefs*, vol. 27, no. 3, pp. 601–604, 2008.
- [22] O. Hoegh-Guldberg, L. R. McCloskey, and L. Muscatine, "Expulsion of zooxanthellae by symbiotic cnidarians from the Red Sea," *Coral Reefs*, vol. 5, no. 4, pp. 201–204, 1987.
- [23] R. J. Jones and D. Yellowlees, "Regulation and control of intracellular algae (= zooxanthellae) in hard corals," *Philosophical Transactions of the Royal Society of London B: Biological Sciences*, vol. 352, no. 1352, pp. 457–468, 1997.
- [24] L. R. McCloskey, T. G. Cove, and E. A. Verde, "Symbiont expulsion from the anemone *Anthopleura elegantissima*," *Journal of Experimental Marine Biology and Ecology*, vol. 195, no. 2, pp. 173–186, 1996.
- [25] C. W. Paxton, S. K. Davy, and V. M. Weis, "Stress and death of cnidarian host cells play a role in cnidarian bleaching," *Journal of Experimental Biology*, vol. 216, no. 15, pp. 2813–2820, 2013.
- [26] J. L. Sachs and T. P. Wilcox, "A shift to parasitism in the jellyfish symbiont *Symbiodinium microadriaticum*," *Proceedings of the Royal Society B: Biological Sciences*, vol. 273, no. 1585, pp. 425–429, 2006.
- [27] T. R. Tivey, J. E. Parkinson, and V. M. Weis, "Host and symbiont cell cycle coordination is mediated by symbiotic state, nutrition, and partner identity in a model cnidarian-dinoflagellate symbiosis," *American Society for Microbiology Host-Microbe Biology*, vol. 11, no. 2, 2020.
- [28] N. Hustedt and D. Durocher, "The control of DNA repair by the cell cycle," *Nature Cell Biology*, vol. 19, no. 1, pp. 1–9, 2017.
- [29] T. P. Neufeld and B. A. Edgar, "Connections between growth and the cell cycle," *Current Opinion in Cell Biology*, vol. 10, no. 6, pp. 784–790, 1998.
- [30] K. W. Orford and D. T. Scadden, "Deconstructing stem cell self-renewal: genetic insights into cell-cycle regulation," *Nature Reviews Genetics*, vol. 9, no. 2, pp. 115–128, 2008.
- [31] A. B. Pardee, "G<sub>1</sub> events and regulation of cell proliferation," *Science*, vol. 246, no. 4930, pp. 603–608, 1989.
- [32] H. Nishitani and Z. Lygerou, "Control of DNA replication licensing in a cell cycle," *Genes to Cells*, vol. 7, no. 6, pp. 523–534, 2002.
- [33] G. R. Stark and W. R. Taylor, "Analyzing the G<sub>2</sub>/M checkpoint," in *Checkpoint Controls and Cancer*, pp. 51–82, Springer, 2004.



- [34] M. Malumbres and M. Barbacid, "Cell cycle, CDKs and cancer: a changing paradigm," *Nature Reviews Cancer*, vol. 9, no. 3, pp. 153–166, 2009.
- [35] W. K. Fitt, "Cellular growth of host and symbiont in a cnidarian-zooxanthellar symbiosis," *The Biological Bulletin*, vol. 198, no. 1, pp. 110–120, 2000.
- [36] E. M. Lehnert, M. E. Mouchka, M. S. Burriesci, N. D. Gallo, J. A. Schwarz, and J. R. Pringle, "Extensive differences in gene expression between symbiotic and aposymbiotic Cnidarians," *Genetics*, vol. 4, no. 2, pp. 277–295, 2014.
- [37] M. Rodriguez-Lanetty, W. S. Phillips, and V. M. Weis, "Transcriptome analysis of a cnidarian–dinoflagellate mutualism reveals complex modulation of host gene expression," *BMC Genomics*, vol. 7, no. 1, p. 23, 2006.
- [38] M. Sorek, Y. Schnytzer, H. W. Ben-Asher et al., "Setting the pace: host rhythmic behaviour and gene expression patterns in the facultatively symbiotic cnidarian *Aiptasia* are determined largely by *Symbiodinium*," *Microbiome*, vol. 6, no. 1, p. 83, 2018.
- [39] D. C. Fingar, C. J. Richardson, A. R. Tee, L. Cheatham, C. Tsou, and J. Blenis, "mTOR controls cell cycle progression through its cell growth effectors S6K1 and 4E-BP1/eukaryotic translation initiation factor 4E," *Molecular and Cellular Biology*, vol. 24, no. 1, pp. 200–216, 2004.
- [40] T. Schmelzle and M. N. Hall, "TOR, a central controller of cell growth," *Cell*, vol. 103, no. 2, pp. 253–262, 2000.
- [41] R. T. Abraham, "Cell cycle checkpoint signaling through the ATM and ATR kinases," *Genes & Development*, vol. 15, no. 17, pp. 2177–2196, 2001.
- [42] S. A. Kitchen, A. Z. Poole, and V. M. Weis, "Sphingolipid metabolism of a sea anemone is altered by the presence of dinoflagellate symbionts," *The Biological Bulletin*, vol. 233, no. 3, pp. 242–254, 2017.
- [43] S. A. Kitchen and V. M. Weis, "The sphingosine rheostat is involved in the cnidarian heat stress response but not necessarily in bleaching," *Journal of Experimental Biology*, vol. 220, no. 9, pp. 1709–1720, 2017.
- [44] S. Baumgarten, M. J. Cziesski, L. Thomas et al., "Evidence for miRNA-mediated modulation of the host transcriptome in cnidarian–dinoflagellate symbiosis," *Molecular Ecology*, vol. 27, no. 2, pp. 403–418, 2018.
- [45] P. Ganot, A. Moya, V. Magnone, D. Allemand, P. Furla, and C. Sabourault, "Adaptations to endosymbiosis in a cnidarian–dinoflagellate association: differential gene expression and specific gene duplications," *PLoS Genetics*, vol. 7, no. 7, p. e1002187, 2011.
- [46] J. L. Matthews, C. M. Crowder, C. A. Oakley et al., "Optimal nutrient exchange and immune responses operate in partner specificity in the cnidarian–dinoflagellate symbiosis," *Proceedings of the National Academy of Sciences*, vol. 114, no. 50, pp. 13194–13199, 2017.
- [47] C. A. Oakley, M. F. Ameismeier, L. Peng, V. M. Weis, A. R. Grossman, and S. K. Davy, "Symbiosis induces widespread changes in the proteome of the model cnidarian *Aiptasia*," *Cellular Microbiology*, vol. 18, no. 7, pp. 1009–1023, 2016.
- [48] S. Baumgarten, O. Simakov, L. Y. Esherick et al., "The genome of *Aiptasia*, a sea anemone model for coral symbiosis," *Proceedings of the National Academy of Sciences*, vol. 112, no. 38, pp. 11893–11898, 2015.
- [49] G. Cui, Y. J. Liew, Y. Li et al., "Host-dependent nitrogen recycling as a mechanism of symbiont control in *Aiptasia*," *PLoS Genetics*, vol. 15, no. 6, p. e1008189, 2019.
- [50] M. J. Cziesski, Y. J. Liew, G. Cui et al., "Multi-omics analysis of thermal stress response in a zooxanthellate cnidarian reveals the importance of associating with thermotolerant symbionts," *Proceedings of the Royal Society B: Biological Sciences*, vol. 285, no. 1877, p. 20172654, 2018.
- [51] N. L. Bray, H. Pimentel, P. Melsted, and L. Pachter, "Near-optimal probabilistic RNA-seq quantification," *Nature Biotechnology*, vol. 34, no. 5, pp. 525–527, 2016.
- [52] H. Pimentel, N. L. Bray, S. Puente, P. Melsted, and L. Pachter, "Differential analysis of RNA-seq incorporating quantification uncertainty," *Nature Methods*, vol. 14, no. 7, pp. 687–690, 2017.
- [53] A. Alexa, J. Rahnenführer, and T. Lengauer, "Improved scoring of functional groups from gene expression data by decorrelating GO graph structure," *Bioinformatics*, vol. 22, no. 13, pp. 1600–1607, 2006.
- [54] E. Quevillon, V. Silventoinen, S. Pillai et al., "InterProScan: protein domains identifier," *Nucleic Acids Research*, vol. 33, no. 2, pp. 116–120, 2005.
- [55] D. Darriba, G. L. Taboada, R. Doallo, and D. Posada, "ProtTest 3: fast selection of best-fit models of protein evolution," *Bioinformatics*, vol. 27, no. 8, pp. 1164–1165, 2011.
- [56] S. Guindon and O. Gascuel, "A simple, fast, and accurate algorithm to estimate large phylogenies by maximum likelihood," *Systematic Biology*, vol. 52, no. 5, pp. 696–704, 2003.
- [57] M. Anisimova and O. Gascuel, "Approximate likelihood-ratio test for branches: a fast, accurate, and powerful alternative," *Systematic Biology*, vol. 55, no. 4, pp. 539–552, 2006.
- [58] S. Guindon, J. F. Dufayard, V. Lefort, M. Anisimova, W. Hordijk, and O. Gascuel, "New algorithms and methods to estimate maximum-likelihood phylogenies: assessing the performance of PhyML 3.0," *Systematic Biology*, vol. 59, no. 3, pp. 307–321, 2010.
- [59] I. Letunic and P. Bork, "Interactive tree of life iTOL v5: an online tool for phylogenetic tree display and annotation," *Nucleic Acids Research*, vol. 49, no. W1, pp. W293–W296, 2021.
- [60] D. J. Thornhill, Y. Xiang, D. T. Pettay, M. Zhong, and S. R. Santos, "Population genetic data of a model symbiotic cnidarian system reveal remarkable symbiotic specificity and vectored introductions across ocean basins," *Molecular Ecology*, vol. 22, no. 17, pp. 4499–4515, 2013.
- [61] D. Fransolet, S. Roberty, A.-C. Herman, L. Tonk, O. Hoegh-Guldberg, and J.-C. Plumier, "Increased cell proliferation and mucocyte density in the sea anemone *Aiptasia pallida* recovering from bleaching," *PLoS One*, vol. 8, no. 5, p. e65015, 2013.
- [62] D. Fransolet, S. Roberty, and J.-C. Plumier, "Impairment of symbiont photosynthesis increases host cell proliferation in the epidermis of the sea anemone *Aiptasia pallida*," *Marine Biology*, vol. 161, no. 8, pp. 1735–1743, 2014.
- [63] C. McQuin, A. Goodman, V. Chernyshev et al., "CellProfiler 3.0: next-generation image processing for biology," *PLoS Biology*, vol. 16, no. 7, p. e2005970, 2018.
- [64] R. C. Team, *R: A Language and Environment for Statistical Computing*, R-Project, 2019.
- [65] A. E. Carpenter, T. R. Jones, M. R. Lamprecht et al., "CellProfiler: image analysis software for identifying and quantifying

- cell phenotypes,” *Genome Biology*, vol. 7, no. 10, pp. R100–R111, 2006.
- [66] A. N. Blackford and S. P. Jackson, “ATM, ATR, and DNA-PK: the trinity at the heart of the DNA damage response,” *Molecular Cell*, vol. 66, no. 6, pp. 801–817, 2017.
- [67] E. R. Kramer, N. Scheuringer, A. V. Podtelejnikov, M. Mann, and J.-M. Peters, “Mitotic regulation of the APC activator proteins CDC20 and CDH1,” *Molecular Biology of the Cell*, vol. 11, no. 5, pp. 1555–1569, 2000.
- [68] A. Golan, Y. Yudkovsky, and A. Hershko, “The cyclin-ubiquitin ligase activity of cyclosome/APC is jointly activated by protein kinases Cdk1-cyclin B and Plk,” *Journal of Biological Chemistry*, vol. 277, no. 18, pp. 15552–15557, 2002.
- [69] L. A. Malureanu, K. B. Jeganathan, M. Hamada, L. Wasilewski, J. Davenport, and J. M. van Deursen, “BubR1 N terminus acts as a soluble inhibitor of cyclin B degradation by APC/CCdc20 in interphase,” *Developmental Cell*, vol. 16, no. 1, pp. 118–131, 2009.
- [70] J. Maciejowski, K. A. George, M.-E. Terret, C. Zhang, K. M. Shokat, and P. V. Jallepalli, “Mps1 directs the assembly of Cdc20 inhibitory complexes during interphase and mitosis to control M phase timing and spindle checkpoint signaling,” *The Journal of Cell Biology*, vol. 190, no. 1, pp. 89–100, 2010.
- [71] V. M. Bolanos-Garcia and T. L. Blundell, “BUB1 and BUBR1: multifaceted kinases of the cell cycle,” *Trends in Biochemical Sciences*, vol. 36, no. 3, pp. 141–150, 2011.
- [72] S. Lee, P. Thebault, L. Freschi et al., “Characterization of spindle checkpoint kinase Mps1 reveals domain with functional and structural similarities to tetratricopeptide repeat motifs of Bub1 and BubR1 checkpoint kinases,” *Journal of Biological Chemistry*, vol. 287, no. 8, pp. 5988–6001, 2012.
- [73] L. Jia, B. Li, and H. Yu, “The Bub1-Plk1 kinase complex promotes spindle checkpoint signalling through Cdc20 phosphorylation,” *Nature Communications*, vol. 7, no. 1, pp. 1–14, 2016.
- [74] R. Visintin, K. Craig, E. S. Hwang, S. Prinz, M. Tyers, and A. Amon, “The phosphatase Cdc14 triggers mitotic exit by reversal of Cdk-dependent phosphorylation,” *Molecular Cell*, vol. 2, no. 6, pp. 709–718, 1998.
- [75] D. O. Morgan, “Regulation of the APC and the exit from mitosis,” *Nature Cell Biology*, vol. 1, no. 2, pp. E47–E53, 1999.
- [76] F. Bassermann, D. Frescas, D. Guardavaccaro, L. Busino, A. Peschiaroli, and M. Pagano, “The Cdc14B-Cdh1-Plk1 axis controls the G<sub>2</sub> DNA-damage-response checkpoint,” *Cell*, vol. 134, no. 2, pp. 256–267, 2008.
- [77] S. C. Bremmer, H. Hall, J. S. Martinez et al., “Cdc14 Phosphatases Preferentially Dephosphorylate a Subset of Cyclin-dependent kinase (Cdk) Sites Containing Phosphoserine,” *Journal of Biological Chemistry*, vol. 287, no. 3, pp. 1662–1669, 2012.
- [78] M. J. R. Stark, S. Hiraga, and A. D. Donaldson, “Protein phosphatases and DNA replication initiation,” in *The Initiation of DNA Replication in Eukaryotes*, pp. 461–477, Springer, 2016.
- [79] O. K. Wong and G. Fang, “CDK1 phosphorylation of BubR1 controls spindle checkpoint arrest and Plk1-mediated formation of the 3F3/2 epitope,” *The Journal of Cell Biology*, vol. 179, no. 4, pp. 611–617, 2007.
- [80] C.-Y. Peng, P. R. Graves, R. S. Thoma, Z. Wu, A. S. Shaw, and H. Piwnicka-Worms, “Mitotic and G<sub>2</sub> checkpoint control: regulation of 14-3-3 protein binding by phosphorylation of Cdc25C on serine-216,” *Science*, vol. 277, no. 5331, pp. 1501–1505, 1997.
- [81] H. C. Reinhardt, P. Hasskamp, I. Schmedding et al., “DNA damage activates a spatially distinct late cytoplasmic cell-cycle checkpoint network controlled by MK2-mediated RNA stabilization,” *Molecular Cell*, vol. 40, no. 1, pp. 34–49, 2010.
- [82] O. Timofeev, O. Cizmecioglu, F. Settele, T. Kempf, and I. Hoffmann, “Cdc25 phosphatases are required for timely assembly of CDK1-cyclin B at the G<sub>2</sub>/M transition,” *Journal of Biological Chemistry*, vol. 285, no. 22, pp. 16978–16990, 2010.
- [83] A. Lindqvist, V. Rodríguez-Bravo, and R. H. Medema, “The decision to enter mitosis: feedback and redundancy in the mitotic entry network,” *Journal of Cell Biology*, vol. 185, no. 2, pp. 193–202, 2009.
- [84] L. Gheghiani, D. Loew, B. Lombard, J. Mansfeld, and O. Gavet, “PLK1 activation in late G<sub>2</sub> sets up commitment to mitosis,” *Cell Reports*, vol. 19, no. 10, pp. 2060–2073, 2017.
- [85] C. Giacinti and A. Giordano, “RB and cell cycle progression,” *Oncogene*, vol. 25, no. 38, pp. 5220–5227, 2006.
- [86] C. V. Dang, “c-Myc target genes involved in cell growth, apoptosis, and metabolism,” *Molecular and Cellular Biology*, vol. 19, no. 1, pp. 1–11, 1999.
- [87] J. van der Sman, N. S. B. Thomas, and E. W.-F. Lam, “Modulation of E2F complexes during G<sub>0</sub> to S phase transition in human primary B-lymphocytes,” *Journal of Biological Chemistry*, vol. 274, no. 17, pp. 12009–12016, 1999.
- [88] H. Tanaka, I. Matsumura, S. Ezoe et al., “E2F1 and c-Myc potentiate apoptosis through inhibition of NF- $\kappa$ B activity that facilitates MnSOD-mediated ROS elimination,” *Molecular Cell*, vol. 9, no. 5, pp. 1017–1029, 2002.
- [89] B. Hoffman and D. A. Liebermann, “Apoptotic signaling by c-MYC,” *Oncogene*, vol. 27, no. 50, pp. 6462–6472, 2008.
- [90] G. Bretones, M. D. Delgado, and J. León, “Myc and cell cycle control,” *Biochimica et Biophysica Acta (BBA)-Gene Regulatory Mechanisms*, vol. 1849, no. 5, pp. 506–516, 2015.
- [91] B. Ren, H. Cam, Y. Takahashi et al., “E2F integrates cell cycle progression with DNA repair, replication, and G<sub>2</sub>/M checkpoints,” *Genes & Development*, vol. 16, no. 2, pp. 245–256, 2002.
- [92] Q. Zhan, M. J. Antinore, X. W. Wang et al., “Association with Cdc2 and inhibition of Cdc2/cyclin B1 kinase activity by the p53-regulated protein Gadd45,” *Oncogene*, vol. 18, no. 18, pp. 2892–2900, 1999.
- [93] J. M. Salvador, J. D. Brown-Clay, and A. J. Fornace, “Gadd45 in stress signaling, cell cycle control, and apoptosis,” in *Gadd45 Stress Sensor Genes*, pp. 1–19, Springer, 2013.
- [94] E. Telles and E. Seto, “Modulation of cell cycle regulators by HDACs,” *Frontiers in Bioscience (Scholar Edition)*, vol. 4, no. 3, pp. 831–839, 2012.
- [95] H. Yan, A. M. Merchant, and B. K. Tye, “Cell cycle-regulated nuclear localization of MCM2 and MCM3, which are required for the initiation of DNA synthesis at chromosomal replication origins in yeast,” *Genes & Development*, vol. 7, no. 11, pp. 2149–2160, 1993.
- [96] C. Liang and B. Stillman, “Persistent initiation of DNA replication and chromatin-bound MCM proteins during the cell cycle in cdc6 mutants,” *Genes & Development*, vol. 11, no. 24, pp. 3375–3386, 1997.

- [97] K. Labib and J. F. X. Diffley, "Is the MCM2-7 complex the eukaryotic DNA replication fork helicase," *Current Opinion in Genetics & Development*, vol. 11, no. 1, pp. 64–70, 2001.
- [98] B. P. Duncker, I. N. Chesnokov, and B. J. McConkey, "The origin recognition complex protein family," *Genome Biology*, vol. 10, no. 3, p. 214, 2009.
- [99] J. Chen, X. Wu, J. Lin, and A. J. Levine, "mdm-2 inhibits the G<sub>1</sub> arrest and apoptosis functions of the p53 tumor suppressor protein," *Molecular and Cellular Biology*, vol. 16, no. 5, pp. 2445–2452, 1996.
- [100] Y. Haupt, R. Maya, A. Kazaz, and M. Oren, "Mdm2 promotes the rapid degradation of p53," *Nature*, vol. 387, no. 6630, pp. 296–299, 1997.
- [101] C. Wasyluk and B. Wasyluk, "Defect in the p53-Mdm2 autoregulatory loop resulting from inactivation of TAFII250 in cell cycle mutant tsBN462 cells," *Molecular and Cellular Biology*, vol. 20, no. 15, pp. 5554–5570, 2000.
- [102] S. S. Clair, L. Giono, S. Varmeh-Ziaie et al., "DNA damage-induced downregulation of Cdc25C is mediated by p53 via two independent mechanisms," *Molecular Cell*, vol. 16, no. 5, pp. 725–736, 2004.
- [103] A. J. Bardin and A. Amon, "MEN and SIN: what's the difference," *Nature Reviews Molecular Cell Biology*, vol. 2, no. 11, pp. 815–826, 2001.
- [104] C. Liang, M. Weinreich, and B. Stillman, "ORC and Cdc6p interact and determine the frequency of initiation of DNA replication in the genome," *Cell*, vol. 81, no. 5, pp. 667–676, 1995.
- [105] J. R. Lipford and S. P. Bell, "Nucleosomes positioned by ORC facilitate the initiation of DNA replication," *Molecular Cell*, vol. 7, no. 1, pp. 21–30, 2001.
- [106] R. M. Golsteyn, K. E. Mundt, A. M. Fry, and E. A. Nigg, "Cell cycle regulation of the activity and subcellular localization of Plk1, a human protein kinase implicated in mitotic spindle function," *The Journal of Cell Biology*, vol. 129, no. 6, pp. 1617–1628, 1995.
- [107] C. J. Sherr and J. M. Roberts, "Inhibitors of mammalian G<sub>1</sub> cyclin-dependent kinases," *Genes & Development*, vol. 9, no. 10, pp. 1149–1163, 1995.
- [108] B. J. Warner, S. W. Blain, J. Seoane, and J. Massagué, "Myc downregulation by transforming growth factor  $\beta$  required for activation of the p15Ink4bG1Arrest pathway," *Molecular and Cellular Biology*, vol. 19, no. 9, pp. 5913–5922, 1999.
- [109] T. Bashir, N. V. Dorrello, V. Amador, D. Guardavaccaro, and M. Pagano, "Control of the SCFSkp2–Cks1 ubiquitin ligase by the APC/CCdh1 ubiquitin ligase," *Nature*, vol. 428, no. 6979, pp. 190–193, 2004.
- [110] H. C. Vodermaier, "APC/C and SCF: controlling each other and the cell cycle," *Current Biology*, vol. 14, no. 18, pp. R787–R796, 2004.
- [111] X. L. Ang and J. W. Harper, "SCF-mediated protein degradation and cell cycle control," *Oncogene*, vol. 24, no. 17, pp. 2860–2870, 2005.
- [112] K. I. Nakayama and K. Nakayama, "Regulation of the cell cycle by SCF-type ubiquitin ligases," in *Seminars in Cell & Developmental Biology*, Academic Press, 2005.
- [113] R. X. Luo, A. A. Postigo, and D. C. Dean, "Rb interacts with histone deacetylase to repress transcription," *Cell*, vol. 92, no. 4, pp. 463–473, 1998.
- [114] K. T. Rogers, P. D. Higgins, M. M. Milla, R. S. Phillips, and J. M. Horowitz, "DP-2, a heterodimeric partner of E2F: identification and characterization of DP-2 proteins expressed in vivo," *Proceedings of the National Academy of Sciences*, vol. 93, no. 15, pp. 7594–7599, 1996.
- [115] H. Siddiqui, D. A. Solomon, R. W. Gunawardena, Y. Wang, and E. S. Knudsen, "Histone deacetylation of RB-responsive promoters: requisite for specific gene repression but dispensable for cell cycle inhibition," *Molecular and Cellular Biology*, vol. 23, no. 21, pp. 7719–7731, 2003.
- [116] H. S. Zhang, A. A. Postigo, and D. C. Dean, "Active transcriptional repression by the Rb-E2F complex mediates G1 arrest triggered by p16<sup>INK4a</sup>, TGF $\beta$ , and contact inhibition," *Cell*, vol. 97, no. 1, pp. 53–61, 1999.
- [117] S. M. Rubin, A.-L. Gall, N. Zheng, and N. P. Pavletich, "Structure of the Rb C-terminal domain bound to E2F1-DP1: a mechanism for phosphorylation-induced E2F release," *Cell*, vol. 123, no. 6, pp. 1093–1106, 2005.
- [118] D. K. Dimova, O. Stevaux, M. V. Frolov, and N. J. Dyson, "Cell cycle-dependent and cell cycle-independent control of transcription by the Drosophila E2F/RB pathway," *Genes & Development*, vol. 17, no. 18, pp. 2308–2320, 2003.
- [119] S. Dalton and L. Whitbread, "Cell cycle-regulated nuclear import and export of Cdc47, a protein essential for initiation of DNA replication in budding yeast," *Proceedings of the National Academy of Sciences*, vol. 92, no. 7, pp. 2514–2518, 1995.
- [120] T. E. Braun, E. Poole, and J. Sinclair, "Depletion of cellular pre-replication complex factors results in increased human cytomegalovirus DNA replication," *PLoS One*, vol. 7, no. 5, p. e36057, 2012.
- [121] L. E. Giono, L. Resnick-Silverman, L. A. Carvajal, S. St Clair, and J. J. Manfredi, "Mdm2 promotes Cdc25C protein degradation and delays cell cycle progression through the G<sub>2</sub>/M phase," *Oncogene*, vol. 36, no. 49, pp. 6762–6773, 2017.
- [122] O. Stevaux and N. J. Dyson, "A revised picture of the E2F transcriptional network and RB function," *Current Opinion in Cell Biology*, vol. 14, no. 6, pp. 684–691, 2002.
- [123] C. Bertoli, J. M. Skotheim, and R. A. M. De Bruin, "Control of cell cycle transcription during G<sub>1</sub> and S phases," *Nature Reviews Molecular Cell Biology*, vol. 14, no. 8, pp. 518–528, 2013.
- [124] H. Kvitt, H. Rosenfeld, and D. Tchernov, "The regulation of thermal stress induced apoptosis in corals reveals high similarities in gene expression and function to higher animals," *Scientific Reports*, vol. 6, no. 1, p. 30359, 2016.
- [125] P. Awasthi, M. Foiani, and A. Kumar, "ATM and ATR signaling at a glance," *Journal of Cell Science*, vol. 128, no. 23, pp. 4255–4262, 2015.
- [126] A. Alexander, S. L. Cai, J. Kim et al., "ATM signals to TSC2 in the cytoplasm to regulate mTORC1 in response to ROS," *Proceedings of the National Academy of Sciences*, vol. 107, no. 9, pp. 4153–4158, 2010.
- [127] C. A. Downs, J. E. Fauth, J. C. Halas, P. Dustan, J. Bemiss, and C. M. Woodley, "Oxidative stress and seasonal coral bleaching," *Free Radical Biology and Medicine*, vol. 33, no. 4, pp. 533–543, 2002.
- [128] B. L. Bingham, J. L. Dimond, and G. Muller-Parker, "Symbiotic state influences life-history strategy of a clonal cnidarian," *Proceedings of the Royal Society of London B: Biological Sciences*, vol. 281, no. 1789, p. 20140548, 2014.
- [129] D. Yellowlees, T. A. V. Rees, and W. Leggat, "Metabolic interactions between algal symbionts and invertebrate hosts," *Plant, Cell & Environment*, vol. 31, no. 5, pp. 679–694, 2008.

- [130] Y. Gabay, V. M. Weis, and S. K. Davy, "Symbiont identity influences patterns of symbiosis establishment, host growth, and asexual reproduction in a model cnidarian-dinoflagellate symbiosis," *The Biological Bulletin*, vol. 234, no. 1, pp. 1–10, 2018.
- [131] M. Habetha, F. Anton-Erxleben, K. Neumann, and T. C. G. Bosch, "The *Hydra viridis* / *Chlorella* symbiosis Growth and sexual differentiation in polyps without symbionts," *Zoology*, vol. 106, no. 2, pp. 101–108, 2003.
- [132] A. Lecointe, I. Domart-Coulon, A. Paris, and A. Meibom, "Cell proliferation and migration during early development of a symbiotic scleractinian coral," *Proceedings of the Royal Society B: Biological Sciences*, vol. 283, no. 1831, 2016.
- [133] Y. J. Passamanek and M. Q. Martindale, "Cell proliferation is necessary for the regeneration of oral structures in the anthozoan cnidarian *Nematostella vectensis*," *BMC Developmental Biology*, vol. 12, no. 1, p. 34, 2012.